Energy & Environmental Science

RSC Publishing

REVIEW

Use of polypyrrole in catalysts for low temperature fuel cells

Cite this: *Energy Environ. Sci.*, 2013, **6**, 1105

Xianxia Yuan,[a] Xin-Long Ding,[a] Chao-Yang Wang*[bc] and Zi-Feng Ma[a]

Received 18th September 2012
Accepted 7th February 2013

DOI: 10.1039/c3ee23520c

www.rsc.org/ees

Carbon materials, especially Vulcan XC-72 carbon black, are the most widely used catalyst support in low temperature fuel cells. Several disadvantages of these catalyst supports, however, limit the catalyst performance leading to reduced fuel cell performance and durability: low resistance to corrosion at high potentials, micropores leading to limited accessible surface, impermeability to gases and liquids, and no proton conductivity. Therefore, development of novel supports or modified carbon materials is essential to commercialization of low temperature fuel cell technology. Due to unique metallic/semiconductor characteristics along with excellent environmental stability, facile synthesis and high conductivity, polypyrrole (PPy), a member of the conjugated heterocyclic conducting polymers, has been considered the most promising alternative to carbon supports in fuel cells. Extensive research on PPy-containing catalysts has been reported in the last twenty years. This paper systematically and critically reviews the progress and main achievements of PPy use in both anode and cathode catalysts for low temperature fuel cells. Insight into the remaining challenges and future research directions is also discussed.

Broader context

Low temperature fuel cells (LTFCs) are promising for future applications to transportation and grid energy storage due to their high energy efficiency and low emissions. Currently, catalysts for LTFCs use carbon supports with inherent limitations in performance and durability. In recent decades, tremendous efforts have been made to seek efficient alternatives to carbon supports, low-cost replacements for precious metal catalysts, and/or novel ionomers for low-platinum loading electrodes without substantial oxygen transport loss, and polypyrrole (PPy) has emerged as a promising and central material with extensive research reported in the literature. While the performance of PPy-containing catalysts is still lower than the targets defined for automotive applications, several recent advances have greatly raised their prospects for fuel cell commercialization and thus prompted significant research and development activities. A comprehensive and critical review on the progress and achievements of PPy-containing catalysts, absent to date, is thus not only timely but also imperative for future research and the practical application in commercial fuel cells. In this review, we summarize the advances garnered on PPy-containing catalysts for LTFCs, identify remaining challenges, and offer research directions in order to further the development of these materials and make the use of PPy in commercialized fuel cells a reality.

1 Introduction

Low temperature fuel cells, such as proton exchange membrane fuel cells (PEMFCs), direct methanol fuel cells (DMFCs), direct ethanol fuel cells (DEFCs) and alkaline membrane fuel cells, represent an environmentally friendly technology that converts chemical energy directly into electricity through electrochemical reactions with high efficiency.[1–3] They have attracted considerable interest in recent years with increasing pollution and depletion of natural energy resources. At present, almost all low temperature fuel cells employ carbon-supported catalysts. In particular, Vulcan XC-72 carbon black is a common choice for supporting nanosized electrocatalyst particles because of its large surface area, high electrical conductivity and suitable pore structure. However, the use of carbon blacks as a fuel cell catalyst support presents some disadvantages.[3–8] First, porous electrically conductive carbon blacks do not exhibit adequate resistance to corrosion caused by electrochemical oxidation. Second, the presence of micropores less than 1 nm in carbon does not permit the fuel supply to the surface to occur smoothly, thus limiting the activity of the catalyst. In the same way, the large number of micropores results in low accessible surface area for the deposition of metal particles, leading to poor catalytic activity. Third, carbon is impermeable to gases and liquids and does not conduct protons, thereby limiting achievable catalyst performance and resulting in low catalyst utilization and reduced fuel cell performance. In order to facilitate transport of protons within the catalyst layer and thereby maximize catalyst utilization, a proton-conducting polymer (*e.g.*,

[a]*Department of Chemical Engineering, Shanghai Jiao Tong University, Shanghai 200240, China*

[b]*Center for Energy Storage and Conversion, Department of Energy and Resources Engineering, Peking University, Beijing 100871, China*

[c]*Electrochemical Engine Center (ECEC), Departments of Chemical Engineering, Mechanical and Nuclear Engineering, and Materials Science and Engineering, The Pennsylvania State University, University Park, Pennsylvania 16802, USA. E-mail: cxw31@psu.edu; Fax: +1-814-863-4848; Tel: +1-814-863-4762*

Nafion solution) is usually mixed with catalysts (Fig. 1a),[9] providing a network binding catalyst particles (*e.g.* Pt). The ideal catalyst support to replace both carbon and Nafion ionomer and provide enhanced performance should be gas and liquid permeable, and should conduct both electrons and protons. Therefore, more robust conducting polymers and conducting metal oxides[10–14] have been attracting much attention as alternative catalyst support materials in low temperature fuel cells.

Conjugated heterocyclic conducting polymers, such as polypyrrole (PPy), polyaniline (PANi), polyacetylene (PA), poly-(3-methylthiophene) (P3MT) and polythiophene (PTh), have received more and more attention since the late 1970s because of their unique metallic/semiconductor characteristics and potential use in areas such as electronics,[15] biosensors and actuators,[16] electrochemistry and electrocatalysis.[17–20] Among these, PPy has been considered the most promising by virtue of its excellent environmental stability, facile synthesis and higher conductivity.[21–25]

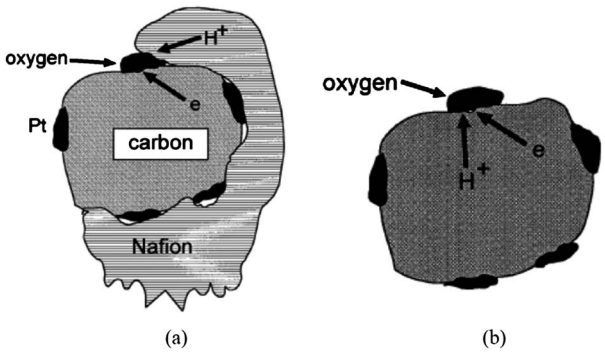

Fig. 1 Pictorial representation of a catalyst layer for (a) a conventional electrode with a carbon support and Nafion, and (b) a novel electrode with PPy as the catalyst support replacing both carbon and Nafion. Reprinted from ref. 9.

PPy is a type of chemical compound formed from a number of connected pyrrole ring structures, giving rise to high electrical conductivity. Since the initial synthesis in 1916,[26] PPy has

Dr Xianxia Yuan is an associate professor in the Department of Chemical Engineering, Shanghai Jiao Tong University (SJTU), China. She received her Ph.D. degree in Material Physics and Chemistry from Shanghai Institute of Microsystem and Information Technology, Chinese Academy of Sciences in 2002, and then joined SJTU. From 2008 through 2009, Dr Yuan worked in the Pennsylvania State University as a visiting scholar along with professor Chao-Yang Wang. She has published about 70 peer-reviewed journal papers, 7 patents, 1 book and 2 book chapters. Dr Yuan's research interest is now focused on fuel cells and lithium-air batteries.

Xin-Long Ding obtained a master's degree in Chemical Engineering at Shanghai Jiao Tong University in March 2011. His thesis was focused on cobalt–polypyrrole catalysts supported on carbon for oxygen reduction reaction in proton exchange membrane fuel cells under the supervision of Dr Xianxia Yuan. He is currently working as a process and piping engineer at Shanghai Keyuan Chemical & Gas Engineering Design Company.

Dr Chao-Yang Wang received his Ph.D. in Mechanical Engineering from the University of Iowa in 1994, and he is currently William E. Diefenderfer Chair in Mechanical Engineering and a Distinguished Professor of Mechanical, Chemical and Materials Engineering at the Pennsylvania State University. Dr Wang's research interests cover the transport, materials, manufacturing and modeling of batteries and fuel cells.

Dr Zi-Feng Ma is currently a distinguished professor of Chemical Engineering and the founding director of the Institute of Electrochemical and Energy Technology at Shanghai Jiao Tong University, China. He received his bachelor and master degrees from Zhejiang University and Ph.D. degree from South China University of Technology. He has made remarkable contributions to new materials for electrochemical energy systems and published over 200 technical papers, 20 patents and 6 book chapters. His research interests are focused on new materials for fuel cells and electrochemical energy storage systems including lithium ion batteries, lithium air batteries and supercapacitors.

become a material of interest to many researchers contributing to several thousand publications and demonstrating numerous applications ranging from energy storage devices to advanced technological applications such as radar absorbing coatings in military defense systems. Extensive work has been done to investigate its fabrication, modification, performance improvement and characterization. In general, PPy can be synthesized by chemical polymerization or electrochemical polymerization. Either method has its own advantages and disadvantages, according to the specific requirements of the application. Chemical polymerization by oxidative agents[27–30] can be successfully applied to supply a great amount of PPy or appropriate PPy structures, and it is easy to prepare PPy particles with different and/or controlled size ranging from several nanometers up to several micrometers and/or containing various inclusions with this method. Electrochemical polymerization[31–33] has found an application as a general deposition method if thin PPy layers are required. By using this method, the thickness and morphology of the deposited layer might be controlled by the application of well-defined potential and known coulombs passing through the electrochemical cell. The capability of electrochemical polymerization could also be significantly extended by using alternative electrochemical processes such as galvanostatic deposition, cyclic voltammetry and potential pulse techniques. Therefore, both PPy synthesis methods are finding particular application areas for various technological requirements.

In recent years, PPy has been employed in major components of low temperature fuel cells, such as membranes,[34–39] bipolar plates[40–44] and electrocatalysts[9,45–47] for performance improvement. In electrocatalysts, PPy is usually used as a catalyst support to replace or partially replace both the generally used carbon support and the polyelectrolyte (such as Nafion) in the catalyst layer, and sometimes directly as metal-free catalysts. A pictorial representation is given in Fig. 1b.[9] When PPy is used, a two-phase boundary in the catalyst layer is sufficient for the electron and proton transport for the electrochemical reaction, as compared to the three-phase boundary when carbon is used as a catalyst support, since PPy is permeable to gases and water, and exhibits both electronic and ionic conductivity.[47] PPy-enabled elimination of ionomers in a fuel cell catalyst layer could offer a new route for using low-Pt loading technology without suffering significant oxygen transport loss through ionomers, thus providing a major possibility for low-cost, commercially viable fuel cells.

The aim of this work is to review major advances and applications of PPy in catalysts for low temperature fuel cells. Pending challenges and future research directions are also identified and discussed.

2 Use of PPy in cathode catalysts for low temperature fuel cells

The reported PPy-containing cathode catalysts for low temperature fuel cells can to date be classified into two groups: metal-free catalysts and metal-containing catalysts. The former are mainly restricted to use in acidic media with very few in alkaline media, while much research on the latter has been reported in both acidic and alkaline media. The metal-containing cathode catalysts in acidic media can be further grouped into Pt- and transition metal-based catalysts, while those in alkaline media are mainly focused on transition metal-based catalysts.

2.1 Metal-free catalysts

In recent years, a large number of metal-free cathode catalysts with improved four-electron-transfer oxygen reduction selectivity and enhanced durability have been reported,[48,49] among which the most developed is nitrogen-doped carbon with phthalocyanine,[50] melamine,[51] pyridine,[52] cyanamide,[53] ammonia,[54] nitrogen gas,[55] as well as PPy[56] as the nitrogen source or the source of both nitrogen and carbon. The state-of-the-art metal-free N-doped carbon materials are considered as a potential substitute for Pt catalysts to substantially reduce the catalyst cost as well as enhance its stability for oxygen reduction reaction (ORR), thus enabling widespread commercialization of low temperature fuel cell technology.

Great disagreement existed in the results about the catalytic ability of PPy itself towards ORR during the 1980s and 1990s. One representative opinion was of Rajeshwar's group from the University of Texas at Arlington.[57,58] They electrochemically prepared a PPy thin film with potentiostatic[57] and potentiodynamic[58] techniques, respectively, in 0.1 M KCl solution containing 0.05 M pyrrole, and found a non-negligible catalytic activity of the obtained PPy towards ORR in 0.05 M H_3PO_4 solution. Similarly, Jakobs *et al.*[59] synthesized a PPy film through an electrochemical potentiostatic method in 0.1 M $LiClO_4$ in acetonitrile solution containing 0.144 M pyrrole, and observed that PPy is electrocatalytically active towards ORR. However, conflicting results were presented by Okabayashi *et al.*[60] who declared that a PPy film has no catalytic activity for any electrode reaction including ORR.

Recent studies on both pristine PPy and pyrolyzed PPy demonstrated strong catalytic activity towards ORR. Wu *et al.*[61] chemically synthesized PPy with ammonium peroxydisulfate (APS) as an oxidant in 1.0 M HCl containing pyrrole, and found that the as-prepared PPy could catalyze ORR in 0.5 M NH_4Cl solution. Khomenko *et al.*[62] obtained PPy by chemical polymerization of 0.5 ml pyrrole with 1.2 g of $FeCl_3$ in 50 ml of 0.1 M HCl, and found that PPy possesses the ability to catalyze the oxygen electroreduction. They proposed that oxygen can interact only with PPy in the reducing state (close to the fully undoped state), and a molecule of oxygen can be adsorbed on the surface of PPy only when both oxygen atoms form bonds with surface carbon atoms, *i.e.* a bridge model of adsorption is probable. Thus-established O–O bond orders in chemisorbed oxygen molecules are lower than those in a free O_2 molecule and a noticeable increase in the O–O bond length takes place during adsorption. As a result, chemisorbed O_2 molecules have a fairly high degree of activation and can be easily reduced by PPy. It is noted that the reported ORR catalytic activity of PPy widely varied from experiment (and/or materials) to experiment and much more fundamental work is still needed to reproduce stable performance.

Generally, micropores in catalysts and/or the support are the greatest contributor to surface area but impede fuel delivery, whereas macropores allow for efficient mass transport but contribute much less surface area for reaction. Thus, mesopores are typically preferred for providing high surface area and allowing efficient mass transport at the same time. In order to obtain a mesoporous metal-free N-doped carbon catalyst with narrow pore size distribution towards ORR, PPy was employed as a source of both nitrogen and carbon to prepare a nanostructured catalyst with the help of ordered mesoporous silica (OMS) as a hard template along with pyrolysis at high temperature as described in Fig. 2.[63] Herein, $FeCl_3$ is used not only as an oxidant for pyrrole polymerization, but also as a catalyst which promotes, during the carbonization stage, the formation of graphitic structures from the amorphous carbon in order to improve the conductivity of the final catalyst.[64,65] Thus the prepared metal-free catalyst CPPy-800 appeared to be a good negative replica of the OMS template, SBA-15, with mesopores centered at 3.3 nm (Fig. 3a). A single ordered structure with long carbon nanorods arranged in a regular pattern (4.7 nm average diameter and 3.3 nm average separation) was observed (Fig. 3b and c). The PPy backbones were converted to mostly graphitic carbon with sp^2 hybridization in CPPy-800 with an unusually high nitrogen content of C/N (atom%) ratio of 8.3, and the CPPy-800 catalyst exhibited clearly enhanced ORR activity (Fig. 3d) as well as corrosion resistance (Fig. 3e and f) as compared to conventionally used Vulcan XC-72 carbon.[63] The authors attributed the ORR enhancement of CPPy-800 to the delocalization of electron at carbon due to nitrogen leading to a weakened O–O bond, but the exact mechanism remains unclear. They ascribed the improved corrosion resistance to the higher graphitization in CPPy-800 as well as the stronger C–N bond than C–C bond due to the higher affinity of nitrogen to water which is the source of oxygen for surface oxidation. The authors, therefore, proposed that it may be possible to make a highly resistant yet active carbon material by tuning the nitrogen functionality and its population.

In general, the morphology/structure–performance relationship is of great importance for developing materials with optimal performance. For PPy as metal-free catalysts for ORR, several studies have comparatively explored the effects of PPy morphology on the ORR catalytic performance, since various PPy morphologies, such as film, powder, sphere, nanofiber, nanowire, nanotube array and so forth, could be synthesized with facile control.[66–73] Wu *et al.* chemically synthesized PPy powder[61] and PPy nanofiber film,[73] respectively, and compared their ORR activity. The results showed that the nanostructured PPy exhibited better ORR performance.[61] PPy with granular- (PPy(g)) and tubules-like (PPy(t)) morphologies was synthesized by Morozan *et al.* using chemical oxidative polymerization with $FeCl_3$ as an oxidant and with/without acid red as a structuring agent, followed by pyrolysis at 800 °C for 2 h in an argon atmosphere to obtain the final metal-free N-doped carbon catalysts PPy(g)/800 and PPy(t)/800.[74] As shown in Fig. 4, the general shape of PPy did not change significantly upon pyrolysis at high temperature under argon, but the average size of the structures obviously decreased. The authors ascribed the change in the local morphology to a different organization of the polymer chains inside the materials. In contrast to the unchanged shape, new structures have been created in PPy(g)/800 and PPy(t)/800 due to denitrogenation reactions during pyrolysis. The nitrogen in PPy(g) and PPy(t) is mainly pyrrolic-N while that in PPy(g)/800 and PPy(t)/800 is mainly distributed between pyridinic-N and quaternary-N (Fig. 5), resulting from

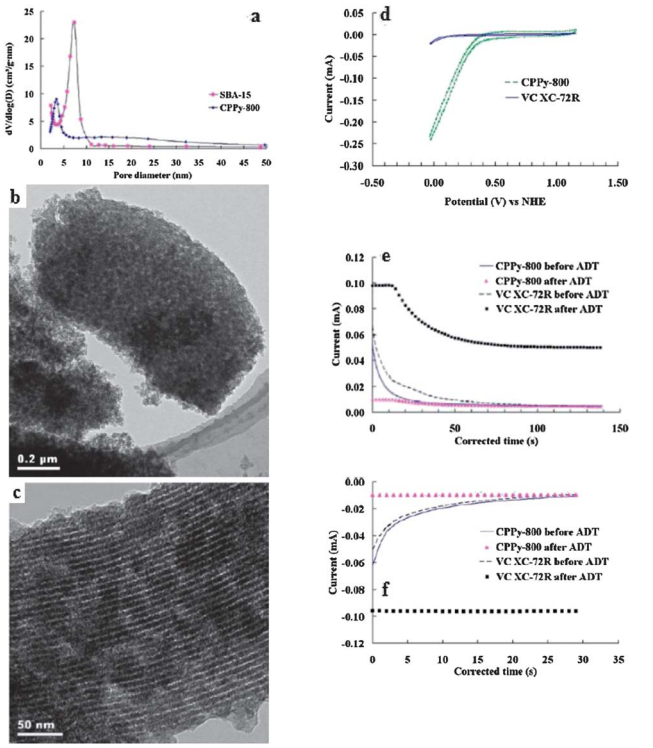

Fig. 3 (a) Pore size distribution of SBA-15 and CPPy-800; (b) TEM images of a particle of CPPy-800; (c) TEM images of the longitudinal section of CPPy-800; (d) ORR polarization curves recorded at 1600 rpm with a 5 mV s^{-1} scan rate for CPPy-800 and VC XC-72R carbon in O_2-saturated 0.5 M H_2SO_4 at 25 °C; (e) chronoamperometric curves before and after accelerated degradation test (ADT) at a potential of 1.4 V *vs.* NHE for CPPy-800 and VC XC-72R carbon in N_2-saturated 0.5 M H_2SO_4; (f) chronoamperometric curves before and after ADT at a potential of 0.1 V *vs.* NHE for CPPy-800 and VC XC-72R carbon in N_2-saturated 0.5 M H_2SO_4. Reprinted from ref. 63.

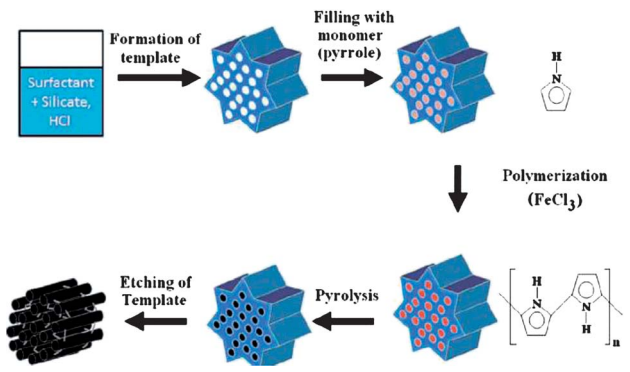

Fig. 2 A schematic for the synthesis of nitrogen functionalized ordered mesoporous carbon. Reprinted from ref. 63.

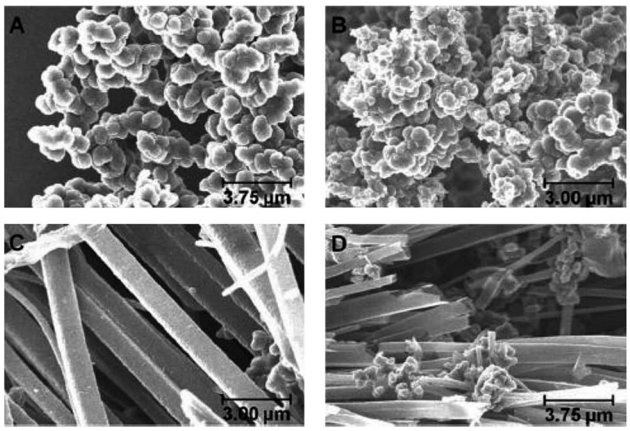

Fig. 4 SEM images of PPy(g) (A), PPy(g)/800 (B), PPy(t) (C) and PPy(t)/800 (D). Reprinted from ref. 74.

the incorporation of a nitrogen atom within a new carbon structure that provides a better coordination with carbon atoms, stabilizing the N-bonded carbon structure into an in-plane functional group stable at higher temperature. Comparative electrochemical studies on PPy(g)/800 and PPy(t)/800 in 0.1 M KOH solution revealed a better ORR performance of the latter, including higher ORR peak potential and peak current, higher ORR onset potential, higher electron transfer number and lower hydrogen peroxide yield, and better stability (Fig. 6). Since the catalytic activity of nitrogen-doped carbon materials in alkaline media was recently related to quaternary-N, while comparable N 1s spectrum composition has been observed for PPy(g)/800 and PPy(t)/800, the authors claimed that the different ORR performance is caused by the structural morphology of PPy and can be explained by the higher electrical conductivity of PPy in the tubular structure than in the granular one. Therefore, the authors proposed that the control of the structural morphology is critical to improve the catalytic activity of annealed polymer catalysts. More experimental confirmation of this explanation is needed.

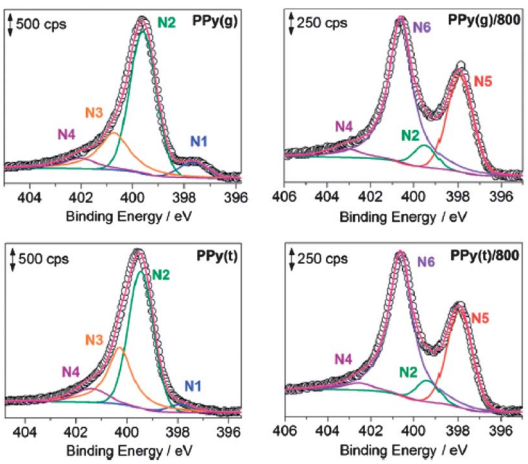

Fig. 5 Deconvoluted XPS N 1s core level spectra of PPy(g), PPy(g)/800, PPy(t) and PPy(t)/800. Reprinted from ref. 74.

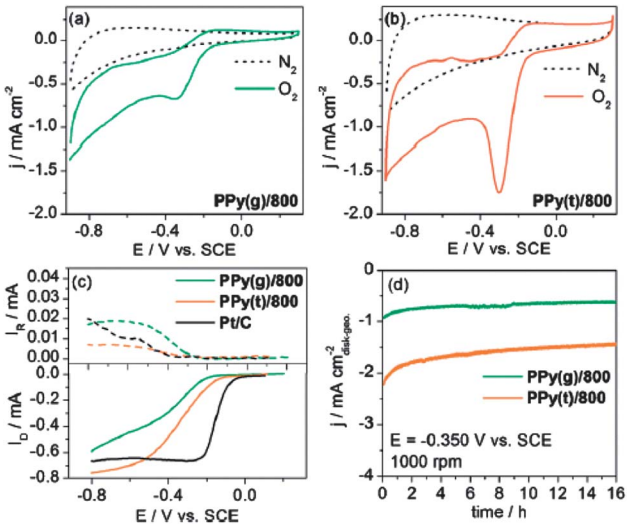

Fig. 6 (a and b) Cyclic voltammograms of PPy(g)/800 and PPy(t)/800 catalysts in 0.1 M KOH electrolyte (scan rate: 20 mV s^{-1}, catalyst loading: 425 μg cm^{-2}); (c) RRDE measurements for PPy(g)/800, PPy(t)/800 and Pt/C catalysts in O_2-saturated 0.1 M KOH. The ring electrode was polarized at 0.456 V (5 mV s^{-1}, 800 rpm); (d) chronoamperometric curve of the ORR on PPy(g)/800 and PPy(t)/800 catalysts in O_2-saturated 0.1 M KOH solution at $E = -0.350$ V *vs.* SCE and 1000 rpm. Reprinted from ref. 74.

In addition, PPy has been used to enhance the electrocatalytic performance of anthraquinones and the derivatives towards ORR. The researchers incorporated the anthraquinones into the PPy matrix as doping species by electropolymerizing pyrrole in a 0.5 M H_2SO_4 aqueous solution containing both pyrrole and anthraquinones[75–77] or sequential electropolymerization of pyrrole and electrodeposition of anthraquinones,[78] and comparative studies demonstrated that the ORR catalytic activity of anthraquinones in acidic media could be apparently improved by reducing the overpotential and enhancing the peak current through immobilizing them into a PPy matrix. It was shown that PPy has little impact on the two-electron-transfer ORR mechanism of anthraquinones, while it is only used as an electron transfer matrix and protective layer for long term stability. PPy can further reduce H_2O_2 into H_2O in a potential range more negative than the one in which the two-electron reduction of oxygen proceeds efficiently on the anthraquinone sites, but its degradation under high H_2O_2 concentration conditions may result in a decrease in the electrocatalytic activity of the composite catalyst.

2.2 Metal-containing catalysts

2.2.1 Metal-containing catalysts in acidic media

2.2.1.1 Pt-based catalysts. The early research on ORR with Pt-based PPy-containing cathode catalysts was mainly focused on dimension dependence of the activity. Vork and Barendrecht[79] synthesized a Pt/PPy catalyst through electrochemical oxidative polymerization of pyrrole followed by electrodeposition of Pt particles, and studied the effects of experimental parameters on the catalytic performance for ORR. It was shown that the ORR activity of the obtained Pt/PPy

catalyst depends strongly upon how the Pt particles are incorporated into the polymer. When Pt particles are deposited with high current density, they are mainly situated near the surface of the PPy layer (*i.e.*, near the polymer/electrolyte interface), leading to a higher conversion rate of O_2 and higher selectivity for the formation of H_2O. In contrast, the Pt particles are much more evenly distributed over the whole PPy film when low current density is used, leading to poor ORR activity and product composition shift to H_2O_2. The authors attributed the results to the different available Pt surface area and oxygen diffusion distance. Similarly, Holdcroft and Funt's investigation[80] of electrochemically prepared PPy-containing Pt microparticles showed that, when Pt is localized at the PPy/O_2 solution interface, the oxygen reduction reaction yields limiting currents which are affected by O_2 solution hydrodynamics only. Conversely, when Pt is homogeneously dispersed in the PPy film, the ORR catalytic current is limited by the rate of O_2 permeation in the PPy film. However, conflicting results were reported by Rajeshwar's group.[57,58] They electrochemically prepared a 3D Pt/PPy catalyst from a solution containing pyrrole and colloidal platinum particles that were apparently "electrotrapped" within the growing polymer matrix, affording a three-dimensional array of the catalyst. Comparative studies were conducted with massive platinum and 2D Pt/PPy which was prepared by electrodepositing Pt islands on top of the PPy film. The results showed that massive Pt and 2D Pt/PPy electrodes have comparable activity at a potential of −400 mV *vs.* SCE (saturated calomel electrode), whereas the 3D Pt/PPy catalyst shows obvious enhancement, and the performance degradation was much more severe for the 2D Pt/PPy than for the 3D Pt/PPy catalyst. The authors attributed this difference to the favorable influence on the PPy electric conductivity when platinum particles are dispersed within its bulk, as in 3D Pt/PPy, and the ORR enhancement on 3D Pt/PPy is likely a manifestation of the fine dispersion of the platinum catalyst particles in the 3D Pt/PPy samples. Besides, this study found that the ORR activity increases with the thickness of the PPy film, which the authors attributed to the microporosity and larger active area in the thicker film wherein the catalytic reaction can take place.

In order to improve proton conductivity of PPy and oxygen permeation, composite particles of PPy/PSS were synthesized by incorporation of polystyrenesulfonate (PSS) into PPy, followed by chemical deposition of Pt particles.[9] The authors found that chemically prepared PPy/PSS has quite different ion transport properties from electrochemically prepared materials, as the former adopts a structure/morphology more suitable for rapid ion (proton) transport. However, Pt deposition, by hydrogen reduction of K_2PtCl_4, resulted in an electrical conductivity change from 3 S cm^{-1} to 0.3 S cm^{-1}, leading to lower open circuit voltage and maximum steady state current density in the polarization curve for ORR, compared to values typically observed with carbon supported catalysts under the same conditions. The authors believed that the inferior performance of the new catalyst is due, at least in part, to the large Pt particle size of 200 nm. However, a small Pt particle size of 2–4 nm, by reduction of $Pt(NH_3)_4Cl_2$ with formaldehyde or oxidation of $Na_6Pt(SO_3)_4$ with H_2O_2, leads to a large decrease of conductivity to 10^{-5} S cm^{-1} because of PPy degradation.[81]

To develop corrosion-resistant catalyst supports as an alternative for conventional carbon supports, Huang *et al.*[82] synthesized PPy *via in situ* chemical oxidative polymerization directed by modified self-degradable templates with sodium dodecyl sulfate as the surfactant. Then, a supported Pt catalyst was prepared by wet reduction of $PtCl_4$ with sodium formate. The electrochemical experiments revealed that the obtained PPy is much more resistive than conventional carbon support, Vulcan XC-72, to oxidation at high positive potential, leading to better electrochemical stability of Pt/PPy than Pt/C. The obtained Pt/PPy catalyst demonstrated good ORR kinetics and comparable fuel cell performance with that of a commercial E-TEK Pt/C catalyst. However, the long-term stability of the PPy support under fuel cell operating conditions is still under study and unclear. In this research, the authors showed that the Pt/PPy catalyst is highly selective for the oxygen reduction reaction *via* a four-electron-transfer process. However, contrary conclusions have been drawn by Mokrane *et al.*[83] They prepared PPy modified carbon by chemical polymerization of pyrrole in a carbon containing solution, followed by deposition of Pt nanoparticles on the surface through the carbonyl chemical route in $Na_2PtCl_6 \cdot 6H_2O$ solution. The comparative study showed that use of PPy changed the oxygen reduction mechanism from a four-electron-transfer reaction with production of H_2O to a two-electron-transfer reaction with H_2O_2 as the product. The larger the PPy content, the more the H_2O_2 produced.

To increase the interfacial conductivity without sacrificing the high surface area and pore volume of OMC (ordered mesoporous carbon), which has been considered a promising catalyst support for low temperature fuel cells because of its appealing structural characteristics, Choi *et al.*[84] selectively modified the outer surface of OMC with PPy by an OMS template as illustrated in Fig. 7. The obtained composite PPy-OMC maintained a regular mesoporous structure and the high surface area of the OMC with electrical resistance decreased by 57% from the value for pristine OMC. When Pt (3 nm, 60 wt%) was deposited on the surface of PPy-OMC by hydrogen reduction of $H_2PtCl_6 \cdot 6H_2O$, the obtained catalyst Pt/PPy-OMC exhibited a much larger electrochemically active surface area than HiSpec 9100, a commercial Johnson Matthey catalyst with the same Pt loading and particle size. The DMFC with Pt/PPy-OMC as a cathode catalyst demonstrated 50% enhanced power density compared to that with HiSpec 9100. The authors ascribed the enhancement to the open mesoporous structure combined with the decreased electrical resistance in the catalyst support.

To improve Pt utilization in the carbon supported catalyst, Unni *et al.*[85] proposed a strategy of polishing the carbon surface by effectively filling a significant amount of micro- and mesopores (which generally make an adverse contribution to the achievement of high Pt utilization) with PPy, followed by depositing Pt particles using the pre-precipitation method. They chemically polymerized a small, controlled amount of pyrrole in a carbon slurry followed by precipitating Pt ions ($(NH_4)_2PtCl_6$) on

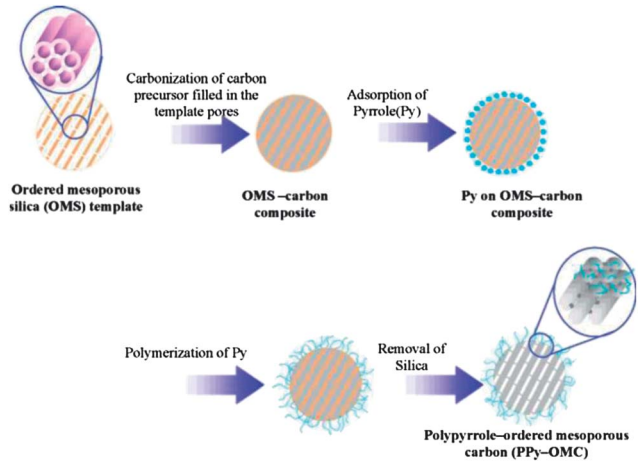

Fig. 7 Outlined representation illustrating the synthesis procedure of ordered mesoporous carbon covered with polypyrrole. Reprinted from ref. 84.

the C–PPy surface and then reduction by $NaBH_4$. Nitrogen adsorption–desorption experiments showed that the obtained composite C–PPy has a decreased surface area (70.4%, from 206 to 61 $m^2 g^{-1}$) and pore volume (58%, from 0.086 to 0.025 $cm^3 g^{-1}$) compared to that of the carbon used. The obtained catalyst Pt/C–PPy–Pre exhibited a larger active surface area of Pt, higher catalytic activity towards ORR and better PEMFC performance compared with Pt/C and Pt/C–PPy wherein the Pt particles were deposited by a general polyol reduction, though the Pt particle size in Pt/C–PPy–Pre is 2 times larger than that in Pt/C and Pt/C–PPy. The authors attributed the enhancement to the fact that the polymer covering of carbon helps both to improve proton and electron transport and to maximize the triple-phase boundary. The relatively smooth surface of PPy filled/covered carbon can assist Pt nanoparticles in dispersing uniformly on the composite with improved adhesion on the surface, while the presence of a heteroatom (nitrogen) in the composite support can reduce the Pt–Pt interatomic distance, prevent platinum particle agglomeration, promote the catalytic activity of Pt nanoparticles and consequently enable high platinum utilization. On the other hand, the pre-precipitation method prevents the passage of nanoparticles into the micro- and mesopores present on the surface due to the formation of colloids during preparation.

Considering that direct polymer coating on carbon may cause some problems, such as lowering the conductivity, blocking the pore structure, agglomerating the carbon particle, and shortening the durability of supports due to the inherent instability of the polymer under harsh operation conditions, Su *et al.*[86] prepared polypyrrole nanospheres (PNs) *via* ultrasonic-assisted chemical polymerization of pyrrole by $FeCl_3$. After carbonization of PNs at 800 °C in a nitrogen atmosphere, the obtained nonporous carbon nanospheres (CNs) were chemically activated by solid NaOH at 900 °C under nitrogen to synthesize N-doped porous carbon nanospheres (PCNs). Then, Pt nanoparticles were deposited on PNs, CNs and PCNs, respectively, as supports to obtain catalysts Pt/PNs, Pt/CNs and Pt/PCNs using ethylene glycol chemical reduction of H_2PtCl_6. The results showed that CNs possess a rougher surface and smaller particles than PNs, while the surface of PCNs looks much coarser than that of CNs. The deposited Pt particles, with an average particle size of about 5 nm, densely covered the surface of PNs, while the Pt nanoparticles were homogeneously dispersed on the surface of CNs and PCNs with sizes of 4–5nm and less than 4 nm, respectively, and the highest dispersion of Pt was found in the catalyst Pt/PCNs. Electrochemical investigation showed that Pt/PNs has negligible catalytic activity towards ORR, while Pt/CNs and Pt/PCNs have evident activity, and Pt/PCNs revealed better performance than the commercial E-Tek Pt/C catalyst. The authors concluded that the inactivity of Pt/PNs is due to the intrinsic resistance of PNs, and the enhanced performance of Pt/PCNs is because of the high dispersion of small Pt nanoparticles on PCNs that possess a developed pore structure, high surface area, and N species.

2.2.1.2 Transition metal-based catalysts. The use of transition metal-based PPy-containing catalysts in cathodes of low temperature fuel cells can be traced back to 1983 by Bull *et al.* from the University of Texas at Austin.[87] They incorporated tetrasulfonated iron phthalocyanines (FePcS) into PPy by electrochemical polymerization of pyrrole in the presence of FePcS onto a glassy carbon electrode, and studied the catalytic performance of the obtained catalyst GC/FePcS/PPy towards ORR in solution with a wide range of pH. They found that incorporation of FePcS into PPy has essentially no effect on the catalytic mechanism, but the conductive property of PPy enhanced the effectiveness of the catalyst by providing more surface area and a larger percentage of active centers than in FePcS without conducting polymers and provided a convenient method of attaching the catalyst to the substrate. According to the authors, the catalyzed oxygen reduction is predominantly into peroxide at low pH, the two- and four-electron-transfer processes compete at intermediate pH, and essentially exclusive reduction of oxygen to water occurs at high pH. However, only very few preliminary studies[88–90] about transition metal-based PPy-containing cathode catalysts could be found during the two decades from 1983.

The research of Yuasa *et al.* published in 2005 (ref. 91) kindled worldwide focus upon transition metal-based PPy-containing cathode catalysts, among which the most studied transition metal is cobalt. They prepared the catalyst, using the procedure shown in Fig. 8,[91] by electropolymerization of pyrrole on the surface of carbon black (CB), followed by suspension in a solution of cobalt acetate in CH_3OH to allow accommodation of cobalt ions at the suitable site. The effects of heat-treatment at 700 °C under a vacuum environment on the catalytic performance of the obtained catalyst CoPPy/CB were comparatively studied in 1 M $HClO_4$ solution. The results showed that heat-treatment could greatly enhance the catalytic activity of CoPPy/CB by positively shifting the half-wave potential, peak potential, plateau current as well as the charge transfer number of the ORR (Figs. 9 and 10), due to the shortened cobalt–cobalt distance in the $Co–N_4$ structure allowing for O_2 molecules to bridge the two proximate cobalt centers. So, the authors showed that surface modification of a carbon particle with PPy provides a simple system allowing the immobilization of cobalt ions at

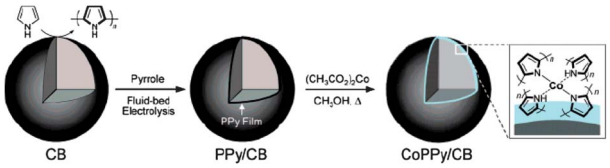

Fig. 8 Schematic of the procedure for preparation of the CoPPy/CB catalyst and the proposed moiety of the catalytic site. Coordination of a single PPy chain as a multidentate ligand is also anticipated. Reprinted from ref. 91.

the surface by coordination processes and displaying electrocatalytic activity for the four-electron-transfer reduction of O_2. In their opinion, the active site for ORR in the studied catalyst is Co–N_4, and the cobalt–nitrogen coordination number might not be changed by the pyrolysis process. Since their work, vast investigation has sprung up concerning the effects of transition metal-based PPy-containing catalysts upon ORR in acidic as well as alkaline media.

The first study that showed PEMFC performance with a Co-based PPy-containing cathode catalyst was reported by Bashyam and Zelenay in 2006.[92] They synthesized a Co–PPy–C catalyst by a pyrolysis-free process consisting of chemical polymerization of pyrrole with H_2O_2 as an oxidant on the surface of Vulcan XC-72 followed by impregnating in $Co(NO_3)_2 \cdot 6H_2O$ solution which was then reduced by $NaBH_4$. This catalyst showed both promising activity and stability without noticeable performance degradation for about 100 h when a backpressure of 2 atm at both sides of the cell was used (Figs. 11 and 12). The H_2–O_2 PEMFC with this material as a cathode catalyst generated about 0.2 A cm^{-2} at 0.50 V and a maximum power density of about

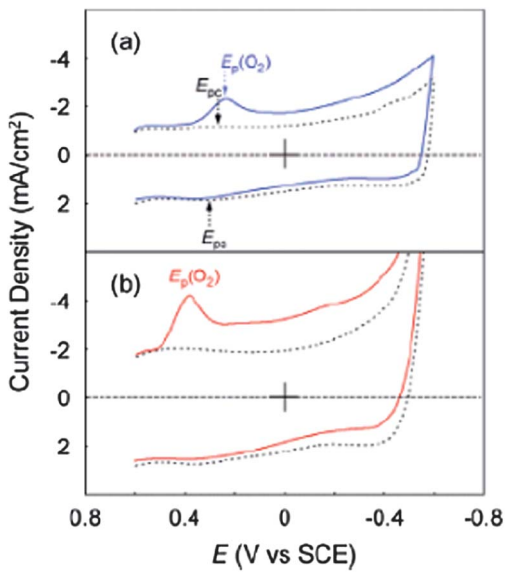

Fig. 9 (a) Cyclic voltammogram for the reduction of O_2 at graphite electrodes coated with the CoPPy/CB catalyst. The modified electrode was prepared by transferring 20 μl of a suspension of CoPPy/CB (2 mg) in 2-propanol containing 5 wt% Nafion (0.25 ml) and was air-dried. The supporting electrolyte, 1 M $HClO_4$, was saturated with O_2 (solid curve) or argon (dotted curve). Scan rate: 0.1 V s^{-1}. (b) Repeat of (a) using the CoPPy/CB catalyst after heat treatment at 700 °C under vacuum. Reprinted from ref. 91.

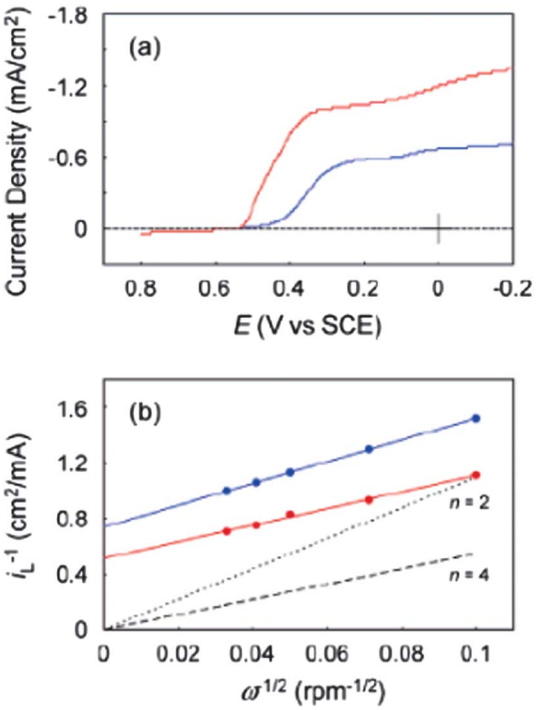

Fig. 10 Current–potential responses for the reduction of O_2 at electrodes in Fig. 9 operated as rotating disk electrodes (electrode rotation rate was 100 rpm) under O_2 (a), and Koutecky–Levich plots (b). Reprinted from ref. 91.

0.14 W cm^{-2}. For a H_2–air PEMFC, the values of current at 0.5 V and peak power density are 0.1 A cm^{-2} and 0.07 W cm^{-2}, respectively, approximately half of that generated with H_2–O_2 PEMFC. The authors suggested that the polymer structure of PPy was retained in the catalyst since no pyrolysis process was used during the catalyst preparation, and the entrapment of the Co sites in the PPy matrix and strong Co–PPy interactions result in the formation of a CoN_x active site that is responsible for ORR. This catalyst synthesis procedure was used by Reddy *et al.* to prepare Co–PPy/MWCNT (MWCNT means multiple wall carbon nanotube) as a cathode catalyst for PEMFCs, DMFCs and DEFCs, except that $FeCl_3$ was employed as an oxidant instead of H_2O_2.[93] The obtained values of current density at 0.5 V and peak power density for PEMFCs at 90 °C are very close to that reported by Bashyam and Zelenay.[92] However, the results are incomparable with those in other reports including ref. 92, since the specific operating conditions for fuel cells haven't been clearly stated. Lee *et al.*[94] prepared the electrocatalyst Co–PPy/C using the same procedure as Bashyam and Zelenay,[92] except replacing Vulcan XC-72 with BP2000, followed by additional pyrolysis at various temperatures under a nitrogen atmosphere. Electrochemical investigation together with physicochemical characterizations showed that additional heat-treatment is of great importance for activity improvement of the catalyst towards ORR and the preferable oxygen reduction mechanism. The ORR catalyzed by the unpyrolyzed Co–PPy/C mainly undergoes a two-electron-transfer pathway, while that by the pyrolyzed catalyst takes parallel reactions of the "series" four-electron peroxide pathway and the "direct" four-electron

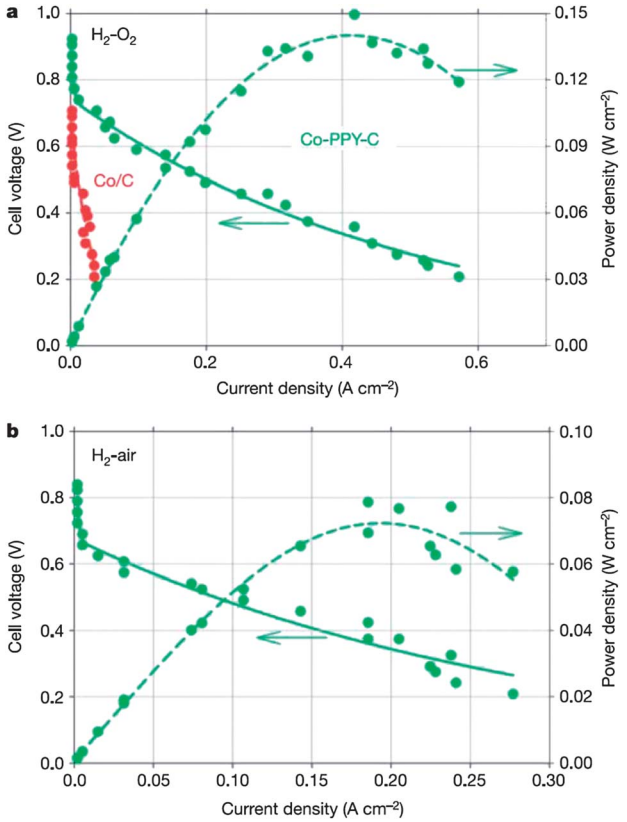

Fig. 11 Fuel-cell performance plots. (a) Polarization and power density plots for H_2–O_2 fuel cells with a Co–PPY–C composite cathode (green lines) and polarization plot for the cell with a Co/C cathode (red line). (b) Polarization and power density plots for H_2–air fuel cells with a Co–PPY–C composite cathode. The Co loading is 6.0×10^{-2} mg cm^{-2}, the cell temperature is 80 °C. Flow rates of hydrogen and oxygen/air at 5 ml s^{-1} and 9 ml s^{-1} (as referred to the standard conditions), respectively. Anode and cathode gases humidified at 90 °C and 80 °C, respectively. The backpressure of gases is 2.0 atm on both sides of the cell. Reprinted from ref. 92.

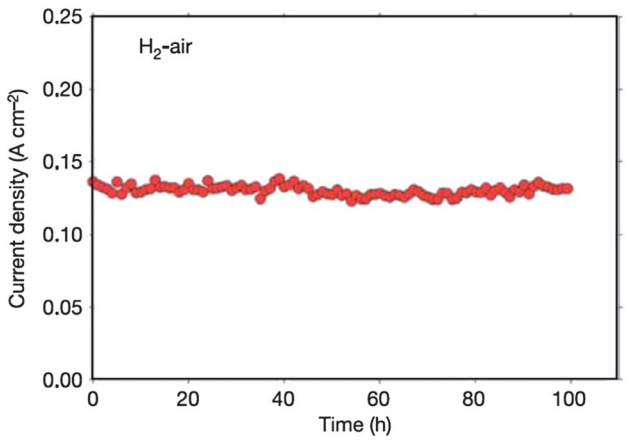

Fig. 12 Durability test of the composite catalyst. Long-term performance of an H_2–air fuel cell with a Co–PPY–C composite cathode at 0.40 V. The Co loading is 6.0×10^{-2} mg cm^{-2}; the cell temperature is 80 °C. Flow rates of hydrogen and air at 5 ml s^{-1} and 9 ml s^{-1} (as referred to the standard conditions), respectively. Anode and cathode gases humidified at 90 °C and 80 °C, respectively. The backpressure of gases is 2.0 atm on both sides of the cell. Reprinted from ref. 92.

pathway. The authors attributed the difference to the fact that Co–N_2 in unpyrolyzed Co–PPy/C is the active site for two-electron-transfer ORR, while pyrrolic (or pyridone) type nitrogen and graphitic nitrogen may be responsible for the enhanced ORR activity and the overall four-electron-transfer mechanism when pyrolyzed Co–PPy/C is used as the catalyst. Therefore, they proposed that heat-treatment is necessary for preparing Co–PPy/C with high catalytic performance towards ORR. Unfortunately, they did not show PEMFC performance with the obtained unpyrolyzed/pyrolyzed Co–PPy/C as a cathode catalyst. This catalyst synthesis technique has been employed, recently, by Thanh *et al.*[95] to prepare Co–PPy/CB electrocatalysts with various CB : Py weight ratios and Co : Py molar ratios. Comparative investigation showed that the composition of Co–PPy/CB catalysts has a major influence on their ORR activity and selectivity, and that the catalyst Co_4–PPy/CB_2 shows the best performance. The possible reasons include the following aspects: a CB : Py weight ratio of 2 allows the deposition and/or incorporation of the highest amount of N on the CB support without oversaturation of the smaller pores needed for the ORR. A Co : Py molar ratio of 4 favors the formation in the catalyst precursor of complexes in which Co is coordinated to 3 or 4 N atoms. Such coordination of Co to N would be at the origin of strong interactions between the concerned atoms, which would limit the formation of low ORR activity Co nanoparticles upon calcination of the precursor. With heat treatment, these Co–N complexes generate CoN_{x-2} sites. The particularly high ORR activity and selectivity of these sites might be due to the coordination of Co that would result in the strong adsorption of O_2 on them, which would promote ORR and restrict peroxide generation. The regret is that no PEMFC performance was shown in this paper even though the authors showed that the best Co_4–PPy/CB_2 catalyst is more than adequate compared with a commercial state-of-the-art Pt catalyst because of the lower H_2O_2 yield in the ORR product.

Yuan *et al.*[96] developed a new synthesis procedure for a Co–PPy/C catalyst by combining those presented by Yuasa *et al.*,[91] Bashyam *et al.*[92] and Lee *et al.*[94] with additional modification. They chemically polymerized pyrrole with APS as an oxidant in a dispersion of BP2000 in isopropyl alcohol, followed by impregnating in $Co(CH_3COO)_2 \cdot 4H_2O$ solution and subsequent heat-treatment in an argon atmosphere at 800 °C. In this procedure, bivalent cobalt in $Co(CH_3COO)_2 \cdot 4H_2O$ was reduced by high temperature pyrolysis instead of $NaBH_4$ solution used by Bashyam and Zelenay[92] and Lee *et al.*,[94] and the polymer structure of PPy has been proven to be destroyed (Fig. 13). The H_2–O_2 PEMFC with the obtained Co–PPy/C as a cathode catalyst delivered a peak power density of 161 mW cm^{-2} without backpressure on either side of the cell (Fig. 14). This value is about 15% higher than that obtained by Bashyam *et al.*[92] using 2 atm backpressure on both sides of the cell. It implies that the synthesis technology is of significant importance for the catalytic performance of Co–PPy/C. However, the exact reason for the performance improvement is still under investigation through a preparation–structure–morphology–performance correlation study and remains unclear at present. In order to further improve the performance of PEMFC with this kind of

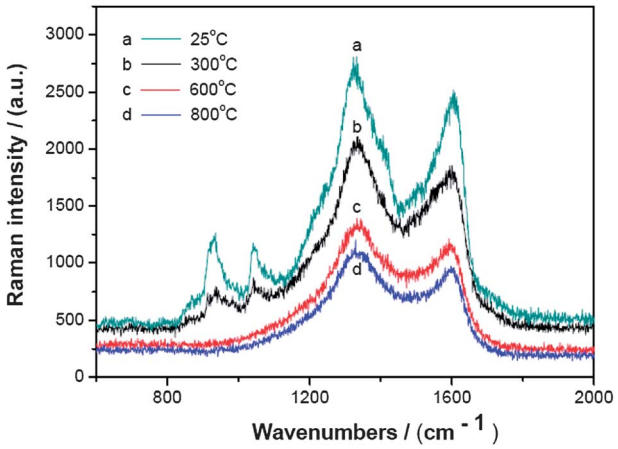

Fig. 13 Raman spectra of Co–PPy/C catalysts heat-treated at various temperatures. Reprinted from ref. 96.

cathode catalyst, *p*-toluenesulfinic acid (TsOH) was introduced during chemical oxidative polymerization of pyrrole. A rotating ring-disk electrode (RRDE) experiment showed that the doped catalyst Co–PPy–TsOH/C is more likely to follow a four-electron-transfer reaction than Co–PPy/C to reduce oxygen directly into H_2O with better electrocatalytic performance (Fig. 15). The resulting PEMFC generated a peak power density of 203 mW cm^{-2} without backpressure used (Fig. 14), which is about 25% higher than that obtained with Co–PPy/C in the same research and about 50% higher than that by Bashyam and Zelenay[92] using 2 atm backpressure on both sides of the cell. This performance currently maintains the worldwide record with Co–PPy/C as a cathode catalyst in PEMFCs. Therefore, the authors suggested that doping TsOH to Co–PPy/C is a valuable way to improve the catalytic activity of Co–PPy/C towards ORR and that Co–PPy–TsOH/C is a promising cathode catalyst for PEMFCs. Yuan *et al.*[96] observed that the content of S in the Co–PPy–TsOH/C catalyst doubled that in Co–PPy/C, although it was not clear whether this is responsible for the enhanced ORR

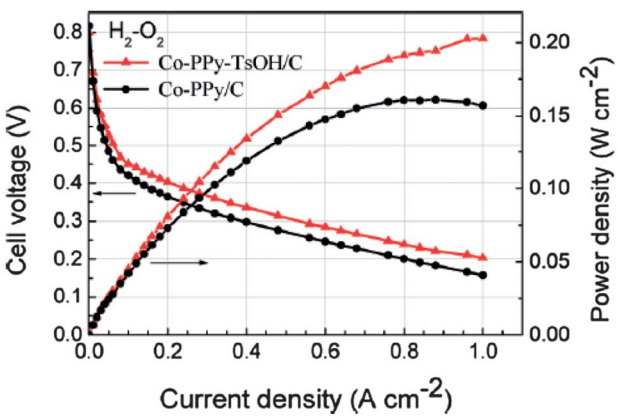

Fig. 14 Polarization and power density curves for H_2–O_2 PEMFCs with commercial Pt (10 wt%)/C as an anode catalyst and Co–PPy/C or Co–PPy–TsOH/C as a cathode catalyst. Conditions: Co loading, 0.35 mg cm^{-2}; Pt loading, 0.15 mg cm^{-2}; cell temperature, 80 °C; flow rate of hydrogen and oxygen, 300 and 540 ml min^{-1}, respectively; anode and cathode reaction gases humidified at 90 and 80 °C, respectively; no backpressure for both sides of the cell. Reprinted from ref. 96.

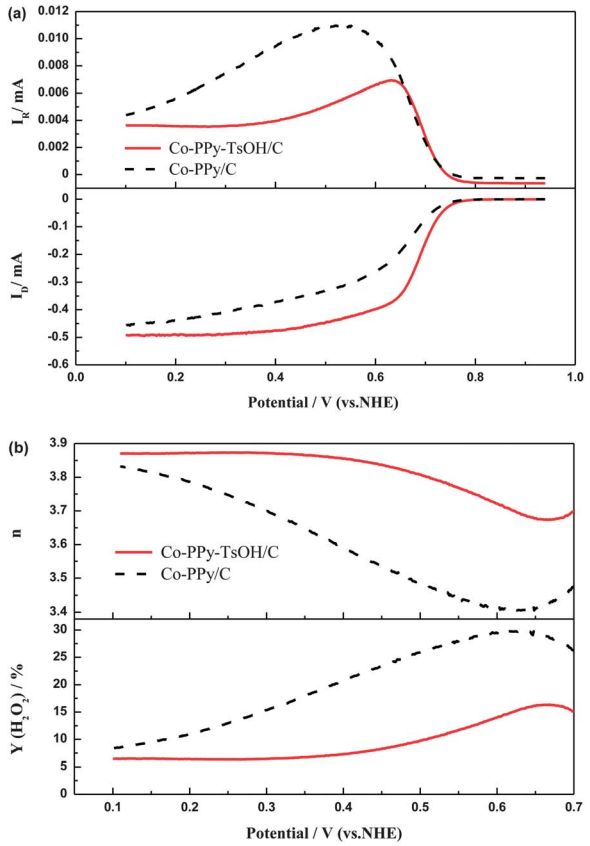

Fig. 15 RRDE voltammograms and the calculated values of transferred electron number (*n*) and yield of H_2O_2 ($Y(H_2O_2)$) during ORR. (a) Polarization curves of Co–PPy/C and Co–PPy–TsOH/C obtained with RRDE at room temperature in O_2 saturated 0.5 M H_2SO_4 with a potential scan rate of 5 mV s^{-1} and an electrode rotation rate of 900 rpm. (b) Calculated values of *n* and $Y(H_2O_2)$ for Co–PPy/C and Co–PPy–TsOH/C catalyzed ORR. Reprinted from ref. 96.

performance. More recently, Feng *et al.*[97] studied the effects of various sulfonate dopants differing mainly in the chain length, including sodium dodecylbenzene sulfonate (DBSNa), sodium *para*-toluene sulfonate (TSNa) and sodium benzene sulfonate (BSNa), on the ORR performance of Co–PPy/C catalysts prepared using the same procedure as ref. 96. They confirmed that sulfo-doping can promote the ORR performance of Co–PPy/C catalysts, and the ORR catalytic performance of the obtained catalysts follows the order DBSNa < TSNa < BSNa. Yuan *et al.*'s synthesis technique has also been employed by Oh *et al.*[98] to develop a highly active and stable Co–PPy/CNF (CNF means carbon nanofiber) cathode catalyst. They found that the use of ethylenediamine (ED) as a chelating agent can greatly improve the performance of Co–PPy/CNF towards ORR. The synthesized Co–ED/PPy–CNF catalyst delivered 0.7 A cm^{-2} at 0.4 V and only 5% performance degradation was observed over 100 h when 2 atm backpressure was used, compared to the values of 0.28 A cm^{-2} and 11% for Co–PPy/CNT. They ascribed the improvement to the synergistic effects of PPy and ED on increasing the total nitrogen content and the contents of specific nitrogen functional groups, such as pyridinic-N and graphitic-N.

Besides, there are some reports about Co-based PPy-containing cathode catalysts to compare the conductive polymers

and their preparation, or to enhance the performance of other catalysts. A class of catalytic nanocomposites based on cobalt, carbon black and heteroatomic polymers including PPy, PANi and P3MT were prepared with the technique reported by Bashyam and Zelenay[92] to be used as cathode materials in PEMFCs.[99] Comparative studies, based on the exchange current densities, the onset potential for ORR and the stability, showed that Co–PPy/C was the material that has the best characteristics for use as a potential fuel cell cathode catalyst, although the onset potential for ORR still needs further improvement. Yuasa *et al.*[100] comparatively studied the effects of preparation techniques of Co–PPy/C as a catalyst for ORR. They found that the contents of Co and N, constituting an active center for ORR, in Co–PPy/C synthesized using the multiple modification method increased remarkably compared with that prepared by electropolymerization of pyrrole followed by suspension in cobalt acetate solution and subsequent heat-treatment,[91] leading to improved catalytic performance towards ORR. In order to improve the catalytic performance of Co–tetraphenylporphyrin (Co–TPP) towards ORR, Chen *et al.*[101] trapped it in a concentrated form within PPy using the standard vapour-phase polymerization technique. The obtained PPy film containing Co–TPP was then deposited onto an ITO (indium tin oxide) glass slide. Electrochemical study indicated that whereas monomeric Co–TPP mainly facilitates two-electron reduction of O_2 to H_2O_2 in open solution or when adsorbed on graphite, it generates predominantly H_2O by four-electron reduction when trapped in a concentrated form within PPy. Similarly prepared PPy–CoTPP deposited onto carbon fiber paper showed excellent activity and stability towards ORR.[102] However, the authors are unclear about the mechanism.

In addition to cobalt, Fe-based, binary-metal-based and mixed valence oxide-based PPy-containing cathode catalysts have also been investigated.

Liu *et al.*[103] synthesized a self-supported iron–polypyrrole mesoporous sphere catalyst (FePPy-MS) by combining the ultrasonic spray pyrolysis technique with the colloidal silica template method (Fig. 16). They chemically prepared PPy with H_2O_2 and $FeCl_3$ as a polymerization oxidant and initiator, respectively, in an aqueous solution made from pyrrole and colloidal silica as a synthetic template. Herein, $FeCl_3$ also acted as an iron precursor. The obtained colloidal solution of PPy and silica was then transferred to an ultrasonic spray pyrolysis system to turn it into aerosol mist that was then carried into a tube furnace by a stream of high-purity nitrogen gas. In the tube furnace, the aerosol droplets were dried, condensed, polymerized, and carbonized at 800 °C. Finally, the silica component in the resulting particles (FePPy–SiO_2 composite particles) was removed by HF etching to obtain the targeted catalyst FePPy-MS. For comparison, they also synthesized a Vulcan XC-72 supported catalyst, FePPy-XC, by chemical oxidative polymerization of pyrrole with H_2O_2 in a solution of XC-72 and potassium ferricyanide followed by heat-treatment at 800 °C and HF etching. Electrochemical experiments of cyclic voltammograms and RRDE showed that much improvement in the activity has been achieved by the self-supporting strategy based on the ORR peak potential, while the charge-transfer number and the amount of hydrogen peroxide as the intermediate for both catalysts are very close to each other, indicating an unchanged ORR mechanism. Real H_2–air PEMFCs with a FePPy-MS catalyzed cathode generated a current density of 0.14 A cm^{-2} at 0.4 V and a maximum power density of 62 mW cm^{-2}, which are 4 and 3.4 times higher than that with FePPy-XC as a cathode catalyst, respectively. The authors attributed the performance improvement to the honeycomb-like mesoporous structure of FePPy-MS, leading to a higher volumetric surface area, active site density and favourable mass transport than in FePPy-XC. Wu *et al.*[104] synthesized PANi–Fe–C and PPy–Fe–C by chemical oxidative polymerization of aniline and pyrrole, respectively, with APS, followed by impregnation in transition metal salts, subsequent heat-treatment in nitrogen, and pre-leaching in 0.5 M H_2SO_4. The comparative investigation with a rotating disk electrode (RDE) and RRDE experiments showed a higher ORR onset potential and better selectivity towards four-electron ORR with PANi–Fe–C than PPy–Fe–C. The PEMFC with PANi–Fe–C demonstrated higher current density at high cell voltage, while PPy–Fe–C showed better performance at lower voltage where oxygen-reduction becomes mass-transport limited. Although the PEMFC with PPy–Fe–C exhibits significantly better performance during the early stage of life test, its performance drops below that of PEMFC with PANi–Fe–C in less than 100 hours. In contrast, PEMFC with PANi–Fe–C demonstrated very good stability during a 200 hour life test. The authors attributed the difference in durability to the different nature in the active ORR sites in the catalysts. They suggest that the aromatic character of aniline is beneficial to stabilizing the interaction of Fe and nitrogen imbedded in the graphitic carbon structure during the heat-treatment, leading to the formation of more stable active sites in PANi–Fe–C.[104,105]

Yuasa *et al.*[106] reported the catalytic performance of CoM–PPy/C (M = Fe or Ir), prepared using the procedure described in ref. 91 towards oxygen reduction reaction. Based on comparative studies on the effects of the atomic ratio of Co/M and heat-treatment and the temperature, they found that a suitable amount of Co replacement with M can shift the ORR peak potential to a

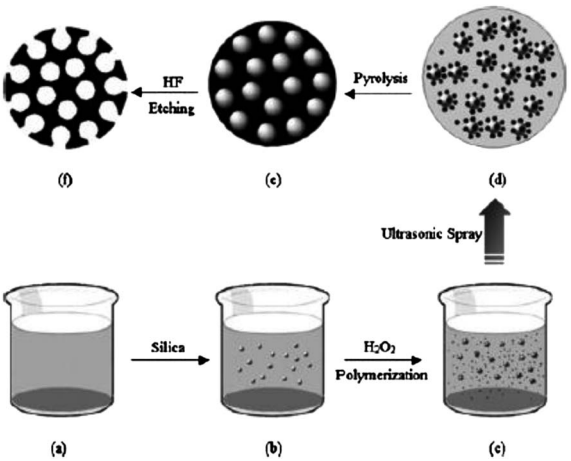

Fig. 16 Schematic illustration of the synthesis process of the FePPy-MS catalyst. Reprinted from ref. 103.

remarkably positive value, and the optimal atomic ratio of Co : Fe is 10 : 1. Their study also revealed that heat-treatment is a beneficial approach to improve the performance of CoM–PPy/C towards ORR, with an optimal heat-treatment temperature for CoFe–PPy/C and CoIr–PPy/C of 650 °C and 600 °C, respectively. In their opinion, the cobalt and M ions were coordinated with nitrogen as the donor atoms in the catalysts. The active sites, metal–N_4 structures, were maintained after the heat treatment under an argon atmosphere without aggregation of metals and formation of alloys. This agrees well with the viewpoint stated in their previous study on the Co–PPy/C catalyst.[91]

Cong *et al.*[107,108] embedded a spinel mixed valence oxide of copper and manganese, $Cu_{1.4}Mn_{1.6}O_4$, into PPy on a glassy carbon (GC) electrode and prepared a composite electrode of GC/PPy/PPy($Cu_{1.4}Mn_{1.6}O_4$)/PPy by a three-consecutive-step electropolymerization technique. Electrochemical studies in KCl + HCl solution with/without oxygen exhibited excellent electrocatalytic reactivity towards ORR with remarkable stability, although the oxide $Cu_{1.4}Mn_{1.6}O_4$ is normally unstable in acidic media. The supposed reason is that the embedding of the oxide particles into the polymer matrix favors the augmentation of the local pH, due to continuous H^+ withdrawal by the ORR and slow interdiffusion of the electrolyte between the sandwich PPy/PPy($Cu_{1.4}Mn_{1.6}O_4$)/PPy layer and the exterior of the composite structure. Therein, they thought that the ORR takes place at $Cu_{1.4}Mn_{1.6}O_4$ particles and the PPy layers play only the role of a charge transporter. Therefore, they suggested that this research introduced a new generation of electrodes for various applications in electrochemistry, involving not only stable electrocatalysts but also unstable electrocatalysts under certain conditions. Based on the understanding that the reactivity of the whole composite electrode depends strongly on the charge transport properties, which are controlled by the electropolymerizing parameters, inside the electrode, the same group also comparatively studied the effects of the doping anions used in the electropolymerization solution on the catalytic reactivity of the PPy/PPy($Cu_{1.4}Mn_{1.6}O_4$)/PPy composite electrode.[109] They found that the nature and concentration of the doping anions have profound effects on the structural characteristics (length of conjugated chains, texture and morphology) and the electrical conductivity of PPy, leading to a determining effect on the ORR performance at PPy/PPy-($Cu_{1.4}Mn_{1.6}O_4$)/PPy composite electrodes, although the ORR takes place at the surface of the oxide nanoparticles. Among the studied anions Cl^-, ClO_4^-, NO_3^-, PF_6^- and SO_4^{2-}, Cl^- was found to be optimal. Therefore, they proposed that an optimization of the various parameters of the PPy electropolymerization and of the oxide preparation might allow researchers to obtain composite electrodes with the highest electrocatalytic reactivity towards ORR.

2.2.1.3 Other catalysts. Other than Pt-based and transition-metal based PPy-containing cathode catalysts, some lanthanides have also been used as the metal component in PPy-containing cathode catalysts. For example, Rajapakse *et al.*[110] introduced PPy into montmorillonite (MMT) type smectite hosts, which have impressive properties such as high cation-exchange capacity, large surface area, Bronsted and Lewis acidity and catalytic properties,[111–113] in order to avoid chain defects such as conjugation interruptions, voids and kinks of conducting polymers leading to poor conductivity of PPy.[114] They prepared Ce(IV) ion-exchanged MMT through a reaction between sodium montmorillonite and $Ce(SO_4)_2$ to widen the interlayers in MMT and change it from hydrophilic to hydrophobic, which is very useful in the polymerization of organic monomers such as pyrrole and aniline in clay.[115] Thus obtained Ce(IV)–MMT was then treated with pyrrole in HCl solution to synthesize Ce(III)–PPy–MMT. During this process, Ce(IV) was used as an oxidant for pyrrole polymerization within the interlayer of MMT. The prepared polymer–clay nanocomposite Ce(III)–PPy–MMT exhibited significant ORR catalytic ability at ambient temperature based on cyclic voltammetry and RDE analysis. Therefore, the authors proposed that the light-weight, durable and stable nanocomposites such as Ce(III)–PPy–MMT will find better applications as cathodes in fuel cells. However, the ORR peak potential of this catalyst, about −0.4 V *vs.* SCE, is much lower than that reported for other efficient catalysts. Therefore, much more attention should be paid to this kind of catalyst to improve its performance, and it will be a long time before it can actually be applied in fuel cells.

2.2.2 Metal-containing catalysts in alkaline media. As discussed above in Section 2.2.1.2, metal-containing PPy was used in cathode catalysts for low temperature fuel cells in alkaline media as early as in 1983.[87] However, widespread attention to the use of PPy in cathode catalysts in alkaline media emerged only in the past ten years.

Hitherto, studies on metal-containing PPy used in cathode catalysts for low temperature fuel cells in alkaline media could be classified into two main groups: transition metal (oxide)-based PPy-containing catalysts and mixed valence oxide-based catalysts.

Extensive research on applications of transition metal (oxide)-based PPy-containing catalysts in alkaline media started in 2007, among which the first was done by Asazawa *et al.*[116] They prepared Co–PPy/C using the same procedure as Bashyam and Zelenay,[92] and here the performance of a direct hydrazine fuel cell (DHFC) with Co–PPy/C as a cathode catalyst was evidently better than that with Ag/C as a catalyst. Qin *et al.*[117] prepared a Co–PPy/C catalyst using the same procedure (with the sole exception that acetylene black was used instead of XC-72), and used it in a direct borohydride fuel cell (DBFC) as a cathode catalyst. Their comparative study revealed that DBFC using a Co–PPy/C cathode demonstrated similar open-circuit voltage and cell performance to that with a Pt/C cathode, with a maximum power density of 65 mW cm^{-2} achieved under ambient conditions. However, long-term stability of the DBFC with the Co–PPy/C cathode was evidently improved from that with traditional catalysts Pt/C and Ag/C. The authors attributed this durability improvement to the observation that the Co atoms in the Co–PPy/C catalyst were linked to pyrrole units to form Co–N bonding without destroying the initial polymer structure (pyrrole ring),[92] and the pyrrole ring would shield Co from the attack of other compounds such as BH_4^-. Olson *et al.*[118] prepared a family of Co–PPy/C catalysts using the procedure of Lee *et al.*,[94] and investigated the effects of Co loading and pyrolysis

temperature on catalytic performance. They found that pyrolysis leads to the formation of a composite catalyst material, featuring Co nanoparticles coated with Co oxides and Co^{2+} species associated with N–C moieties that originate from the PPy structures. The ORR catalytic activity of non-heat-treated Co–PPy/C in oxygen saturated 1.0 M KOH is dependent on Co loading in the catalyst, while it is Co loading independent for the pyrolyzed catalysts. Based on XPS analysis and RRDE experiments in O_2 saturated KOH solution, they established structure-to-property correlations, with principal component analysis (PCA), which suggested a dual-site series ORR mechanism that occurs on pyrolyzed CoPPy/C materials in alkaline media (Fig. 17). Therein, Co–PPy/C catalysts have two distinct classes of active surface species, the Co–N_x site and the Co_xO_y/Co decorated nanoparticle phase. The former is responsible for the initial adsorption of an O_2 molecule and conversion of it to HO_2^- by a two-electron reduction reaction (eqn (1)). Thus formed HO_2^- species can further react at the Co_xO_y/Co decorated site *via* either electrochemical reduction to form OH^- (eqn (2)) or chemical deprotonation to form OH^- and O_2 (eqn (3)). At present, the authors are unclear which of these possible reactions is occurring, but they believed that the decorated Co_xO_y/Co nanoparticle phase is the site of HO_2^- destruction, and that it is strongly linked with the decrease in the flux of HO_2^- species.

$$O_2 + H_2O + 2e^- \rightarrow HO_2^- + OH^- \quad (1)$$

$$HO_2^- + H_2O + 2e^- \rightarrow 3OH^- \quad (2)$$

$$2HO_2^- \rightarrow O_2 + 2OH^- \quad (3)$$

Li *et al.*[119] synthesized a series of M-doped PPy-modified BP2000 catalysts (M = Mn, Fe, Co, Ni, and Cu) with various anion salts by chemical polymerization of pyrrole with H_2O_2 as an oxidant, followed by hydrothermal reaction with metal salts in an incubator at 60 °C. They found that the pyrrole ring was not parallel to the particle surfaces of PPy, and that hydrothermal metal-doping treatment reconfigured PPy by changing the surface nitrogen type/content and releasing the NH proton to form a N–M–N bond and create more catalytic sites. As a result, the ORR performance of the studied catalysts follows the trend, with respect to the transition metal, Co > Cu > Ni > Mn > Fe. Moreover, the doping anion plays an important role in improving the ORR kinetics and pathway due to the fact that when Co^{2+} ions combined with N of PPy to form M–N_x, the corresponding anions were then incorporated onto PPy to change the layered structures of the PPy backbone and the electrical conductivity, thereby affecting electrocatalysis of ORR. Among the studied Co–PPy/BP catalysts prepared with various cobalt salts, that from $Co(NO_3)_2$ exhibited the best ORR performance while that from $CoSO_4$ was the worst. By correlating the electrochemical characteristics and the microstructure of the synthesized M–PPy/BP catalysts, it was concluded that the individual interactions between the carbon support and PPy, carbon support and metal, and metal and PPy are not critical to the enhancement of ORR, while the cooperative interaction (synergy) among the metal, N (from PPy), and C (from BP2000) is the key towards improving ORR kinetics.

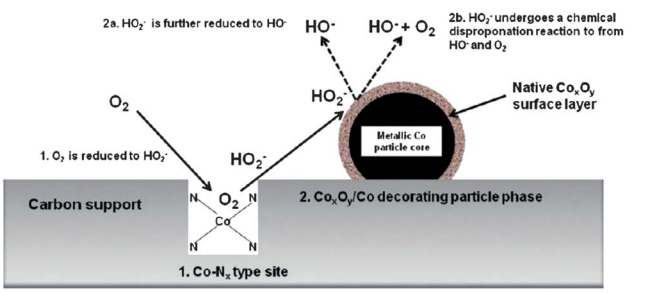

Fig. 17 Model of the active pyrolyzed Co–PPy/C catalyst surface. The active surface species and the ORR mechanistic processes that they support are included. Reprinted from ref. 118.

Qin *et al.* prepared $Co(OH)_2$–PPy/C catalysts[120–122] since they found, in their previous research,[117] that the chemical valence of cobalt in Co–PPy/C prepared using Bashyam and Zelenay's procedure[92] was +2 but not zero. They synthesized the catalyst through traditional chemical oxidative polymerization of pyrrole with H_2O_2 as an oxidant onto the surface of carbon powder, followed by impregnating in $Co(NO_3)_2$ solution and the subsequent chemical (but not redox) reaction with NaOH. When acetylene black was employed as the carbon support,[120] the DBFC with $Co(OH)_2$–PPy/C in both the cathode and anode demonstrated a maximum power density of 83 mW cm^{-2} which was about 4 times higher than that using a PPy-free $Co(OH)_2$/C catalyst. When $Co(OH)_2$–PPy/C and Zr–Zn composite are used as cathode and anode catalysts, respectively, and humidified oxygen is used in the cathode as an oxidant[121] instead of dry oxygen as in the literature,[120] a peak power density of about 250 mW cm^{-2} was achieved. They attributed the performance improvement from the $Co(OH)_2$/C catalyst to the decrease of ohmic resistance and the increase of electrical conductivity of the cathode electrode resulting from PPy modification, since they believed that DBFC performance is dominated by cathode polarization but not anode polarization. However, a comparison with the previous work of the same authors[117] revealed that the performance stability of DBFC with $Co(OH)_2$–PPy/C as a cathode catalyst is obviously poorer than that with Co–PPy/C, although higher peak power density has been achieved with a single cell experiment. The authors could not completely understand this phenomenon, but they suggested the possibility that $Co(OH)_2$ in the catalyst was oxidized into $CoHO_2$ during DBFC operation.

In order to further improve the electrocatalytic activity of $Co(OH)_2$–PPy/C as used in the cathode of DBFC, Qin *et al.*[121] studied the effects of heat treatment, in the temperature range from 400 °C to 800 °C, on the composition, structure and morphology as well as the catalytic performance of the catalyst. They found that $Co(OH)_2$ in the catalyst decomposes into different/multi-component cobalt oxides during pyrolysis at various temperatures under a N_2 atmosphere, and the best catalytic performance obtained by heat-treatment at 600 °C can be attributed to the multi-phase formation of CoO, Co_3O_4 and metallic Co with a platelet shape (which is beneficial to ORR). This opinion agrees well with the results in the literature[123,124] that oxygen reduction overpotential could be effectively

decreased by using cobalt mixed oxides with different valence states due to the synergetic effect. However, the formation of a spheroidal Co composite and the increase of crystallization degree at 800 °C led to the deterioration in electrocatalytic activity towards ORR as well as the decrease of the electron-transfer number during the ORR. Qin *et al.*[122] also comparatively studied the effects of super P (SP) and BP2000 as a carbon support in $Co(OH)_2$–PPy/C, prepared using the same procedure as in the literature,[120] on its properties as a catalyst for DBFC. The results showed that the carbon support has notable influences on the morphology and electrocatalytic activity of $Co(OH)_2$–PPy/C when used as a cathode catalyst in DBFC. The maximum power density of 160 mW cm^{-2} achieved with DBFC using $Co(OH)_2$–PPy-BP in both the anode and cathode was 28% higher than that of the cell with $Co(OH)_2$–PPy-SP (126 mW cm^{-2}). They attributed this difference to the larger specific surface area of BP2000 than super P carbon, resulting in a higher PPy content, more homogeneous distribution of $Co(OH)_2$ and faster kinetics of ORR in the catalyst $Co(OH)_2$–PPy-BP.

Mixed valence oxide-based PPy-containing cathode catalysts in alkaline media were mainly studied by Chartier from Université Louis Pasteur in France and his collaborators in Chile and India. As discussed above in Section 2.2.1.2, they prepared a sandwich structure composite electrode PPy/PPy(O_x)/PPy (O_x is $Ni_xCo_{3-x}O_4$, $CoFe_2O_4$, $LaNiO_3$, or $La_{1-x}Sr_xMnO_3$) by embedding a spinel mixed valence oxide into polymer layers with a three-consecutive-step electropolymerization technique, and studied the catalytic performance towards ORR in a mixed aqueous solution of KCl + KOH with various electrochemical and physicochemical techniques.[124–130] The results revealed that the composite electrode modified neither the charge transfer/transport behaviors in the electrical conducting polymer PPy, nor the electrocatalytic activity of the oxide, but it exhibited higher electrocatalytic reactivity towards ORR and excellent operating stability in alkaline media without dissolution of oxide and chemical overoxidation of PPy, although HO_2^- is generated during the catalyzed ORR. The authors gave an explanation that the external layers of the composite electrode protect the oxide, and the produced H_2O_2 is chemically decomposed in the space of the confinement of the oxide particles limiting the yield of H_2O_2 in the electrolyte. Therefore, the authors proposed that this kind of a triple-layer composite electrode prepared by embedding a mixed valance oxide into electronically conductive polymers is a class of promising catalysts for ORR in alkaline media. Improvement and optimization are envisioned through proper choice of the oxide, the doping anion, and the dispersion medium for the oxide.

3 Use of PPy in anode catalysts for low temperature fuel cells

PPy-containing catalysts used in the anode of low temperature fuel cells are mainly metal-containing catalysts for hydrogen and methanol oxidation, and relatively little research has been reported for the oxidation of other small organic molecules, such as ethanol[131] and formic acid,[132,133] as fuels in low temperature fuel cells.

3.1 Metal-containing catalysts for hydrogen oxidation

The studies on metal-containing PPy catalysts for anodic hydrogen oxidation in low temperature fuel cells are mainly concentrated on the electrochemical preparations. In 1993, Chen *et al.*[57] electrochemically prepared a three-dimensional Pt/PPy catalyst from a solution containing pyrrole and colloidal platinum particles. This catalyst exhibited a remarkable enhancement (5 times) in activity for hydrogen oxidation reaction (HOR) relative to a massive platinum comparison standard, while with an increase in the PPy film thickness and the platinum loading, the number of transferred electrons for the HOR approached the limiting value of 2 as observed for the massive Pt. The authors could not fully understand this result since PPy itself has negligible catalytic activity towards HOR, but they presumed that perhaps a catalyst–polymer synergic interaction played a positive role in the catalytic enhancement. Vork *et al.*[134] comparatively studied the catalytic properties of Pt/PPy prepared by electrochemically depositing platinum particles on a PPy covered glassy carbon disc and the incorporation of Pt particles during the polymerization of pyrrole on a glassy carbon disc towards hydrogen oxidation. They found that the Pt/PPy prepared using the former method exhibits good catalytic behaviour, while the inclusion of Pt particles, despite higher Pt loading, during polymerization of pyrrole leads to a catalyst with much lower activity. They ascribed this result to the low availability of Pt surface which was covered with PPy in the catalyst synthesized by the latter technique. In this work, the catalysts with poly(*N*-methylpyrrole) and polyaniline as the conducting polymer were also prepared, by the former technique, with the catalyzed hydrogen oxidation starting at a much higher potential than that with PPy, although similar diffusion limited behaviour was observed. The most recent study on Pt/PPy catalysts for hydrogen oxidation was conducted by Bouzek *et al.*[135] They prepared Pt/PPy catalysts using three different methods: (i) cathodic deposition of platinum from a hexachloroplatinum complex $[PtCl_6]_2$ on the pre-synthesised polymer film, (ii) incorporation of colloidal platinum particles into the polymer film during electropolymerization and (iii) incorporation of a tetrachloro–platinum complex $[PtCl_4]^{2-}$ during the electropolymerization as the counter ion and subsequent cathodic reduction. The authors compared these methods with respect to the distribution of platinum in the polymer film and the catalytic activity of the composite for the hydrogen oxidation reaction. The results showed that a real three-dimensional homogeneous distribution of Pt microparticles inside PPy cannot be obtained by method (i), while methods (ii) and (iii) should be employed to achieve this. The highest Pt loading inside PPy was obtained by method (iii), but such a catalyst manifested much lower catalytic activity for the hydrogen oxidation reaction in comparison to the catalysts prepared by the other two methods that exhibited electrocatalytic activities comparable to that of bare Pt electrodes. It is worth noting that this result is contrary to that of Vork *et al.*[134] as discussed above, since they revealed that the catalyst prepared using method (i) has better catalytic performance than that using method (ii) towards HOR. The probable reasons for this discrepancy lie, at

least in part, in the different preparation techniques/parameters for PPy and Pt particles, and the diverse Pt precursors. On the other hand, both studies[134,135] presented the opinion that hydrogen oxidation is limited by the amount of Pt on the catalyst surface, but not in the interior of the film.

There are also studies in the literature reporting inferior performance of PPy as a support of Pt catalysts for hydrogen oxidation reaction. For example, Bouzek *et al.*[136] electrochemically synthesized PPy followed by electrodeposition of Pt, in which the study of the obtained catalyst Pt/PPy towards HOR showed that the application of PPy film as a catalyst support has no advantage over commercially available carbon supported catalysts. The authors thought that the main reason is the low permeability of PPy for fuel and water, since it limits the catalyst utilization on its surface and disturbs water management in the fuel cell.

PPy has also been used as the support of Pd to prepare an anodic catalyst for hydrogen oxidation reaction. Seo *et al.*[137] electrochemically fabricated a Pd/PPy catalyst in a layer-by-layer manner, and compared its catalytic performance towards HOR with a non-PPy, namely bare Pd, catalyst. In their study, Pd showed rapid deactivation caused by the formation of surface Pd oxide species and dissolution of Pd to the electrolyte, while the electrochemical catalytic stability examined from a half-cell test as well as actual fuel cell operation was significantly improved when Pd/PPy was used in the anode. The authors attributed the stability enhancement to the features of the conducting polymer like redox property *via* interacting with H^+ and/or OH^- and its capability of storing and transporting charge, which can suppress the oxidative deactivation of active Pd sites and impede particle agglomeration.

3.2 Metal-containing catalysts for methanol oxidation

As early as in 1992, PPy was introduced into an anode catalyst towards methanol oxidation reaction (MOR) by Strike *et al.*[138,139] They electrochemically prepared a PPy thin film by cyclic voltammetric polymerization, followed by electrodeposition of a small amount of dispersed Pt particles. The comparative investigation showed that incorporation of Pt particles inside PPy leads to radical improvement in catalytic activity and durability in contrast with bulk Pt metal or Pt dispersed on other supports, and that the obtained Pt/PPy composite apparently does not undergo poisoning even in the course of prolonged oxidation runs. Their study also revealed that the thickness of PPy in the range from 100 to 700 nm does not affect the catalytic behavior of the Pt/PPy catalyst, whilst Pt loading in the catalyst has a considerable influence, such that the rising Pt content leads to enhanced activity. Similarly, Becerik and Kadirgan[132] electrochemically polymerized PPy at a constant potential followed by electrodeposition of Pt particles. The obtained catalyst Pt/PPy revealed improved catalytic performance over pure Pt towards MOR, with its activity depending greatly on the deposition potential of Pt, and a value of about −0.46 V *vs.* mercury/mercury sulphate (MSE) electrode was found to be the optimal polymerizing potential. Radhakrishnan and Adhikari[140] developed metal halides doped PPy as a catalyst for methanol oxidation by electropolymerization of pyrrole followed by de-doping in 1 M NH_3 solution and then doping in an aqueous solution of the corresponding chloride with concentrations ranging from 0 to 20 mM. The comparative study showed that the electronegativity of the dopant ion plays a very important role in the electrocatalytic activity of the obtained catalyst wherein a decrease in electronegativity of the dopant ions causes an increase in the catalytic performance. An activity trend of $ZrCl_4 > PdCl_2 > MnCl_2 > FeCl_3 > CoCl_2 > CuCl_2 > NiCl_2$ was found for the studied dopants.

As discussed in Section 2.2.1.1, Su *et al.*[86] chemically synthesized PNs followed by carbonization and KOH etching at high temperature to obtain CNs and PCNs, respectively, in order to overcome the disadvantages of directly coating the carbon surface with PPy. The electrochemical study on Pt deposited PNs, CNs and PCNs as the catalyst support showed that Pt/PNs is inactive towards MOR because of the low conductivity of PNs. Though a similar onset potential for methanol oxidation has been found for catalysts Pt/PCN, Pt/CN and an E-Tek commercial Pt/C catalyst, Pt/PCN exhibited the highest mass activity and the lowest oxidation peak potential, and Pt/CN showed comparable mass activity to that of a commercial E-Tek catalyst but with a higher oxidation potential that is undesired. The authors attributed the excellent performance of Pt/PCNs to the high dispersion of small Pt nanoparticles on PCNs that possess a developed pore structure, high surface area, and N species. Similar work was done by Ma *et al.*,[141] who chemically polymerized pyrrole into PPy nanowires followed by decomposition at 800 °C under an Ar atmosphere to obtain CN_x nanofibers, after which Pt nanoparticles were chemically supported on CN_x nanofibers by the microwave-polyol method. The comparative study on the catalytic performance for methanol oxidation, with Pt/XC-72 and Pt/PPy prepared using the same procedure by replacing CN_x with XC-72 and PPy, showed that the catalytic activity follows the order Pt/PPy > Pt/CN_x > Pt/XC-72 (Fig. 18), matching well with the order of the electrochemical active area. The CO tolerance (the ratio of forward peak current to backward peak current in Fig. 18) follows the order Pt/XC-72 > Pt/CN_x > Pt/PPy, matching well with the order of the average Pt particle size in the catalysts (Fig. 19). Electrochemical stability evaluation with cyclic voltammetries before and after immersing the thin film electrodes in the electrolyte for one to four days revealed that both Pt/CN_x and Pt/XC-72 are quite stable, while Pt/PPy degrades seriously. Therefore, they concluded that Pt/CN_x shows the best comprehensive performance and the potential applications in DMFC. In their opinion, Pt particle size in a catalyst is greatly dependent on nitrogen concentration in the support as an active site for nucleation and growth of Pt nanocrystals. The CO tolerance of a catalyst is dependent on Pt particle size, and larger Pt nanoparticles lead to higher CO tolerance. Better catalytic performance not only comes from a larger electrochemical area and smaller Pt size, but also from the modified chemical state of the Pt species by PPy, probably due to the influence of abundant pyrrolic nitrogen, while the deterioration of Pt/PPy is due to degradation of PPy nanowires rather than CO poisoning.

However, there is also literature that reported inferior performance of PPy as the support of an anode catalyst towards

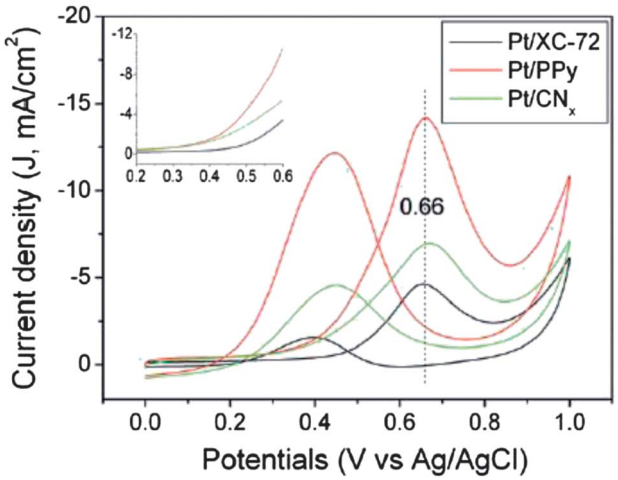

Fig. 18 Cyclic voltammetries of Pt/CN_x (green), Pt/PPy (red) and Pt/XC-72 (black) catalysts in 1 M H_2SO_4 aqueous solution with 1 M CH_3OH. The inset is the forward parts of the CV curves. Reprinted from ref. 141.

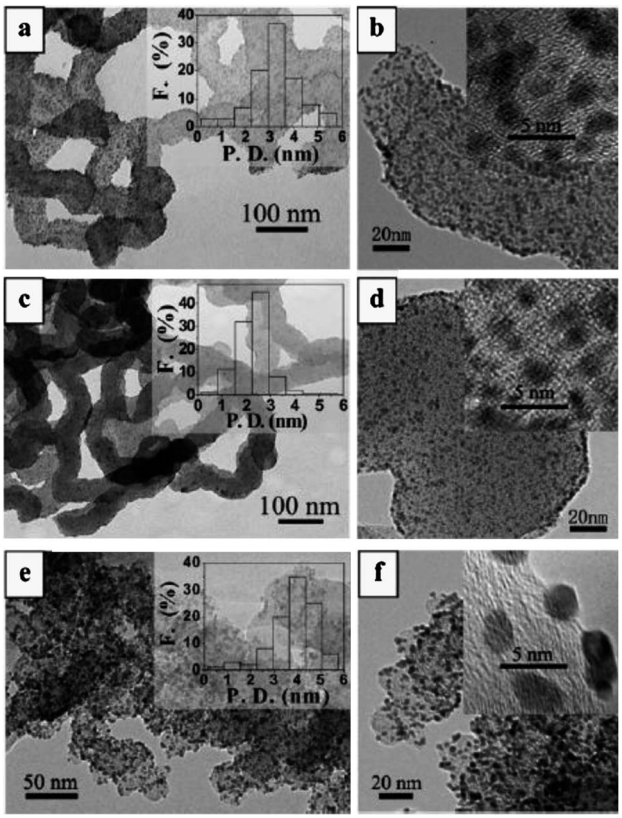

Fig. 19 Typical TEM and HRTEM images of Pt/CN_x, Pt/PPy and Pt/XC-72 catalysts. (a) and (b) for Pt/CN_x, (c) and (d) for Pt/PPy, (e) and (f) for Pt/XC-72. Insets in (a), (c) and (e) are the corresponding size distribution histograms of Pt nanoparticles for each catalyst based on observation of 300 particles, in which P. D. means particle diameter and *F* denotes frequency. Insets in (b), (d) and (f) are the enlarged images. Reprinted from ref. 141.

methanol oxidation. For example, Park *et al.*[142] chemically prepared PPy with different polymerizing oxidants, including $FeCl_3$, APS and O_2, followed by electrochemical deposition of Pt on it. In this study, the Pt/PPy catalyst with oxygen as an oxidant showed a relatively lower activity, while the highest activity was obtained when $FeCl_3$ was used as an oxidant. However, all the obtained Pt/PPy catalysts revealed much poorer performance than the conventional carbon supported Pt catalyst, though comparable stability was obtained. Considering that the morphology of the supporting polymer and the physicochemical state of the catalyst deposited on it play dominant roles in the catalytic activity, the authors attributed the inferior performance of the prepared Pt/PPy catalyst mainly to the narrower surface area of the synthesized PPy and the larger particle size of Pt that was electrodeposited on the PPy. Therefore, they suggested that the smooth and high porous polymer matrix with a small and uniform platinum dispersion over its surface is recommended in order to enhance performance.

To improve the performance of a PPy-containing anode catalyst for methanol oxidation, a composite support composed of PPy and carbon has been developed. Zhao *et al.*[143] and Zhang *et al.*[144] prepared a PPy–XC-72 composite support by *in situ* chemical polymerization of PPy on XC-72 followed by chemical deposition of Pt particles on the surface. Both studies revealed that the obtained catalyst Pt/PPy–XC-72 demonstrates higher catalytic activity for methanol oxidation, better CO tolerant ability and long-term stability compared with a commercial Pt/C catalyst[143] and Pt/XC-72 prepared with the same technique.[144] Zhao *et al.* attributed the enhancement to the fact that nanostructured and mixed-conducting PPy in the composite support is favorable for setting up an effective conducting network for electron and proton transportation and may improve the surface morphology for platinum deposition.[143] Zhang *et al.* reasoned that the performance enhancement resulted from pyridinic nitrogen sites in PPy which might provide the main initial nucleation sites for the formation of Pt nanoparticles, leading to smaller Pt particles and higher dispersion in Pt/PPy–XC-72 than in Pt/XC-72. They suggested that the Pt–pyridinic nitrogen sites in Pt/PPy–XC-72 suppress the poisoning CO adsorption on Pt nanoparticles and facilitate the methanol electrocatalytic oxidation.[144] In addition, Zhao *et al.*'s investigation[143] also affirmed that β-naphthalene sulfonic acid (NSA) as a dopant for pyrrole polymerization can obviously improve the MOR catalytic performance of Pt/PPy–XC-72. They thought that this is mainly due to the conductivity enhancement of the catalyst layer resulting from NSA doping in the PPy–XC-72 support. Selvaraj and Alagar[145] and Qu *et al.*[146] prepared PPy-MWNTs composite support by *in situ* chemical polymerization of PPy on the surface of MWNTs as the matrix material, followed by chemical deposition of Pt particles. Selvaraj and Alagar[145] indicated that the presence of MWCNTs leads to higher activity, which might be due to the unique structure of MWCNTs, with an increase of electrochemically accessible surface areas from the synergistic effect of polymers and carbon nanotubes, and with increased electrical conductivity and easier charge-transfer at polymer/electrolyte interfaces allowing higher dispersion and utilization of the deposited Pt nanoparticles. Qu *et al.*[146] attributed the better catalytic stability of Pt/PPy-MWCNTs than Pt/MWCNTs, including the manifested CO-tolerance ability and stable methanol oxidation electroactivation, to the following reasons: first, the existence of PPy actuates the adsorption of

water so as to generate active oxygen species [Pt(M)–OH_{ads}], which induces the easy conversion of Pt–CO_{ads} to CO_2 desorbing away. Second, PPy in the composite support improves the dispersion of Pt particles and the larger amount of Pt(111) face, which is beneficial to improving the catalytic stability and reducing the adsorption sites for CO poisons. Third, more Pt particles were exposed to the surface of the Pt/PPy-MWCNTs catalyst after electrochemical over-oxidation sweep. Finally, PPy promotes CH_3OH and H_2O Langmuir adsorption on the catalyst surface.

In addition, some PPy-containing bimetallic catalysts, such as Pt–Ru/PPy–C, Pt–Fe/PPy–C and Pt–Co/PPy–C, have also been investigated for electrooxidation of methanol. Selvaraj and Alagar[147] and Zhao *et al.*[148] prepared a Pt–Ru/PPy-MWCNTs catalyst by chemical polymerization of PPy on MWCNTs followed by coprecipitation of Pt and Ru with a chemical reduction reaction. In both studies, the obtained Pt–Ru/PPy-MWCNTs catalysts exhibited apparently enhanced catalytic performance (including onset potential, forward peak current density, ratio of forward current to backward current and long-term stability) towards methanol oxidation compared to that of Pt–Ru catalysts with only carbon materials, such as MWCNTs, XC-72, or carbon fibers, as the support. The authors suggested that the improved performance resulted from the smaller particle size and well dispersed PtRu alloy nanoparticles in the catalyst. Zhao *et al.* synthesized Pt–Fe/PPy–XC-72 (ref. 149) and Pt–Co/PPy-MWCNTs[150] through chemical polymerization of pyrrole followed by co-deposition of metals with chemical reduction. The obtained catalyst Pt–Fe/PPy–XC-72 exhibited improved catalytic activity towards methanol oxidation (judging from the onset potential and the peak current density) compared to that of the Pt/PPy–XC-72 catalyst, while its durability was slightly poorer than that of the latter. The authors ascribed the enhanced activity to the uniform dispersion and high utilization of Pt nanoparticles in the PPy-containing catalyst. On the other hand, Zhao *et al.* have compared the MOR catalytic performance of Pt–Co/PPy-MWCNTs with that of Pt–Ru/PPy-MWCNTs, considering that PtRu is the widely accepted most efficient catalyst for methanol oxidation. The results revealed poorer performance than the latter, judging from the onset potential, the peak current density and the CO tolerant ability. However, improved performance, better than that of Pt–Ru/PPy-MWCNTs, was achieved by electrochemical over-oxidation of the Pt–Co/PPy-MWCNTs catalyst. The proposed reason was that the over-oxidation process changed the arrangement and structure of the PPy matrix leading to more Pt–Co particles exposed to the catalyst surface.

4 Concluding remarks

As a member of conjugated heterocyclic conducting polymers, PPy has received great attention and has been widely used in key components of low temperature fuel cells, especially the electrocatalysts, due to the unique metallic/semiconductor characteristics, excellent environmental benignity, facile synthesis and high conductivity. However, there are still many unanswered questions for applying PPy in fuel cell catalysts. First, there existed many controversial results in the literature, indicative of a lack of the knowledge to prepare efficient PPy-containing catalysts for stable and reproducible performance. Second, little attention has been paid to the relationship between the morphology and electrocatalytic performance of PPy-containing catalysts with and without metals. Third, it remains unknown which structure is preferred for high activity catalysts: is it the intrinsic pyrrole-ring structure or the pyrolyzed M–N_x phase? All prior studies on anode catalysts were focused on pyrolysis-free PPy with the pyrrole-ring structure, whereas those on cathode catalysts involved both pristine and heat-treated PPy and offered different interpretations about the preferred structure and active sites. No systematic and comparative work has been done to clarify the preferred PPy structure for either electrode. Fourth, the true functionality of PPy in metal-containing catalysts is still under debate. Does it work as a catalyst support only or as both a support and an active site? What is the fundamental mechanism by which it improves catalytic performance of PPy-modified-carbon supported catalysts? Fifth, the aging mechanism of all PPy-containing catalysts remains largely unknown. Finally, the mechanical properties of PPy and the long-term stability and potential dependence of PPy's conductivity may influence its actual property during fuel cell operation, but no fuel cell scientists and technologists have paid much attention to it. In summary, there are still many pending challenges regarding the use of PPy in catalysts for low temperature fuel cells. Only when these issues are well understood and resolved, can the strategy of using PPy to enhance the performance of both catalysts and the corresponding low temperature fuel cells be fully evaluated.

Acknowledgements

The authors are grateful for the financial support of this work by the National Science Foundation of China (21176155, 20776085) and the STCSM of China (10JC1406900). The support to CY Wang is provided by PKU Center for Energy Storage and Conversion.

Notes and references

1 P. Costamagna and S. Srinivasan, *J. Power Sources*, 2001, **102**, 242–252.
2 X. Ren, P. Zelenay, S. Thomas, J. Davey and S. Gottesfeld, *J. Power Sources*, 2000, **86**, 111–116.
3 E. Antolini, *Appl. Catal., B*, 2009, **88**, 1–24.
4 E. Antolini and E. R. Gonzalez, *Appl. Catal., A*, 2009, **365**, 1–19.
5 K. H. Kangasniemi, D. A. Condit and T. D. Jarvi, *J. Electrochem. Soc.*, 2004, **151**, 125–132.
6 R. L. Borup, J. R. Davey, F. H. Garzon, D. L. Wood and M. A. Inbody, *J. Power Sources*, 2006, **163**, 76–81.
7 J. Wang, G. Yin, Y. Shao, S. Zhang, Z. Wang and Y. Gao, *J. Power Sources*, 2007, **171**, 331–339.
8 L. Li, Y. M. Zhang, J. F. Drillet, R. Dittmeyer and K. M. Juttner, *Chem. Eng. J.*, 2007, **133**, 113–119.

9 Z. G. Qi, M. C. Lefebvre and P. G. Pickup, *J. Electroanal. Chem.*, 1998, **459**, 9–14.
10 T. Ioroi, Z. Siroma, N. Fujiwara, S.-i. Yamazaki and K. Yasuda, *Electrochem. Commun.*, 2005, **7**, 183–188.
11 H. Chhina, S. Campbell and O. Kesler, *J. Power Sources*, 2006, **161**, 893–900.
12 J. W. Long, R. M. Stroud, K. E. Swider-Lyons and D. R. Rolison, *J. Phys. Chem. B*, 2000, **104**, 9772–9776.
13 L. Jang, L. Colmenares, Z. Jusys, G. Q. Sun and R. J. Behm, *Electrochim. Acta*, 2007, **53**, 377–389.
14 K.-W. Park, K.-S. Ahn, Y.-C. Nah, J.-H. Choi and Y.-E. Sung, *J. Phys. Chem. B*, 2003, **107**, 4352–4355.
15 K. Gurunathan, A. V. Murugan, R. Marimuthu, U. P. Mulik and D. P. Amalnerkar, *Mater. Chem. Phys.*, 1999, **61**, 173–191.
16 J. W. Schultze and H. Karabulut, *Electrochim. Acta*, 2005, **50**, 1739–1745.
17 M. A. Careema, Y. Velmurugu, S. Skaarup and K. West, *J. Power Sources*, 2006, **159**, 210–214.
18 V. G. Khomenko, V. Z. Barsukov and A. S. Katashinskii, *Electrochim. Acta*, 2005, **50**, 1675–1683.
19 N. Alonso-Vante, S. Cattarin and M. Musiani, *J. Electroanal. Chem.*, 2000, **481**, 200–207.
20 E. K. W. Lai, P. D. Beattie and S. Holdcroft, *Synth. Met.*, 1997, **84**, 87–88.
21 F. Faridbod, M. R. Ganjali, R. Dinarvand and P. Norouzi, *Sensors*, 2008, **8**, 2331–2412.
22 K. Arshak, V. Velusamy, O. Korostynska, K. Oliwa-Stasiak and C. Adley, *IEEE Sens. J.*, 2009, **9**, 1942–1951.
23 A. H. Chen, K. Kamata, M. Nakagawa, T. Iyoda, H. Q. Wang and X. Y. Li, *J. Phys. Chem. B*, 2005, **109**, 18283–18288.
24 C. F. Zhou, S. Kumar, C. D. Doyle and J. M. Tour, *Chem. Mater.*, 2005, **17**, 1997–2002.
25 L. X. Wang, X. G. Li and Y. L. Yang, *React. Funct. Polym.*, 2001, **47**, 125–139.
26 A. Angeli, *Gazz. Chim. Ital.*, 1916, **46**, 279–283.
27 B. Deore, Z. Chen and T. Nagaoka, *Anal. Sci.*, 1999, **15**, 827–828.
28 M. C. Henry, C. C. Hsueh, B. P. Timko and M. S. Freunda, *J. Electrochem. Soc.*, 2001, **148**, 155–162.
29 A. Ramanavicius, A. Kausaite and A. Ramanaviciene, *Sens. Actuators, B*, 2005, **532**, 111–112.
30 R. Pokrop, M. Zagorska, M. Kulik, B. I. Kulszewicz, B. Dufour, P. Rannou, A. Pron, E. Gondek and J. Sanetra, *Mol. Cryst. Liq. Cryst.*, 2004, **415**, 93–104.
31 H. L. Schmidt, F. Gutberlet and W. Schuhmann, *Sens. Actuators, B*, 1993, **13**, 366–371.
32 K. Habermüller and W. Schuhmann, *Electroanalysis*, 1998, **10**, 1281–1284.
33 W. Schuhmann, C. Kranz, H. Wohlschläger and J. Strohmeier, *Biosens. Bioelectron.*, 1997, **12**, 1157–1167.
34 J. Zhu, R. R. Sattler, A. Garsuch, O. Yepez and P. G. Pickup, *Electrochim. Acta*, 2006, **51**, 4052–4060.
35 E. B. Easton, B. L. Langsdorf, J. A. Hughes, J. Sultan, Z. G. Qi, A. Kaufman and P. G. Pickup, *J. Electrochem. Soc.*, 2003, **150**, 735–739.
36 F. Xu, C. Innocent, B. Bonnet, D. J. Jones and J. Roziere, *Fuel Cells*, 2005, **5**, 398–405.
37 H. S. Park, Y. J. Kim, W. H. Hong and H. K. Lee, *J. Membr. Sci.*, 2006, **272**, 28–36.
38 H. D. Lin, C. J. Zhao, W. J. Ma, H. T. Li and H. Na, *Int. J. Hydrogen Energy*, 2009, **34**, 9795–9801.
39 H. S. Park, Y. J. Kim, W. H. Hong, Y. S. Choi and H. K. Lee, *Macromolecules*, 2005, **38**, 2289–2295.
40 P. Herrasti and P. Ocón, *Appl. Surf. Sci.*, 2001, **172**, 276–284.
41 S. Joseph, J. C. McClure, R. Chianelli, P. Pich and P. J. Sebastian, *Int. J. Hydrogen Energy*, 2005, **30**, 1339–1344.
42 Y. Wang and D. O. Northwood, *J. Power Sources*, 2006, **163**, 500–508.
43 Y. Wang and D. O. Northwood, *J. Power Sources*, 2008, **175**, 40–48.
44 M. A. L. Garcia and M. A. Smit, *J. Power Sources*, 2006, **158**, 397–402.
45 H. Laborde, J. M. Léger and C. Lamy, *J. Appl. Electrochem.*, 1994, **24**, 219–226.
46 H. Lee, J. Kim, J. Park, Y. Joe and T. Lee, *J. Power Sources*, 2004, **131**, 188–193.
47 F. Bensebaa, A. A. Farah, D. S. Wang, C. Bock, X. M. Du, J. Kung and Y. LePage, *J. Phys. Chem. B*, 2005, **109**, 15339–15344.
48 Y. Zheng, Y. Jiao, M. Jaroniec, Y. Jin and S. Z. Qiao, *Small*, 2012, **8**, 3550–3566.
49 D. Yu, E. Nagelli, F. Du and L. Dai, *J. Phys. Chem. Lett.*, 2010, **1**, 2165–2173.
50 R. L. Arechederra, K. Artyushkova, P. Atanassov and S. D. Minteer, *ACS Appl. Mater. Interfaces*, 2010, **2**, 3295–3302.
51 J. Ozaki, N. Kimura, T. Anahara and A. Oya, *Carbon*, 2007, **45**, 1847–1853.
52 Z. Chen, D. Higgins and Z. Chen, *Carbon*, 2010, **48**, 3057–3065.
53 Y. Zheng, Y. Jiao, J. Chen, J. Liu, J. Liang, A. Du, W. Zhang, Z. Zhu, S. C. Smith, M. Jaroniec, G. Q. Lu and S. Z. Qiao, *J. Am. Chem. Soc.*, 2011, **133**, 20116–20119.
54 L. Qu, Y. Liu, J.-B. Baek and L. Dai, *ACS Nano*, 2010, **4**, 1321–1326.
55 J. P. McClure, J. D. Thornton, R. Jiang, D. Chu, J. J. Cuomo and P. Fedkiw, *J. Electrochem. Soc.*, 2012, **159**, F733–F742.
56 S. Shrestha and W. E. Mustain, *J. Electrochem. Soc.*, 2010, **157**, B1665–B1672.
57 C. C. Chen, C. S. C. Bose and K. Rajeshwar, *J. Electroanal. Chem.*, 1993, **350**, 161–176.
58 C. S. C. Bose and K. Rajeshwar, *J. Electroanal. Chem.*, 1992, **333**, 235–256.
59 R. C. Jakobs, L. J. J. Janssen and E. Barendrecht, *Electrochim. Acta*, 1985, **30**, 1433–1439.
60 K. Okabayashi, O. Ikeda and H. Tamura, *J. Chem. Soc., Chem. Commun.*, 1983, 684–685.
61 A. Wu, E. C. Venancio and A. G. MacDiarmid, *Synth. Met.*, 2007, **157**, 303–310.
62 V. G. Khomenko, V. Z. Barsukov and A. S. Katashinskii, *Electrochim. Acta*, 2005, **50**, 1675–1683.

63 S. Shrestha and W. E. Mustain, *J. Electrochem. Soc.*, 2010, **157**, B1665–B1672.
64 C.-M. Yang, C. Weidenthaler, B. Spliethoff, M. Mayanna and F. Schüth, *Chem. Mater.*, 2005, **17**, 355–358.
65 A. B. Fuertes and T. A. Centeno, *J. Mater. Chem.*, 2005, **15**, 1079–1083.
66 Y. Han, Q. Zhang, F. Han, C. Li, J. Sun and Y. Lu, *Polymer*, 2012, **53**, 2599–2603.
67 J. Jang and H. Yoon, *Langmuir*, 2005, **21**, 11484–11489.
68 X. Zhang, J. Zhang, W. Song and Z. Liu, *J. Phys. Chem. B*, 2006, **110**, 1158–1165.
69 X. Zhang and S. K. Manohar, *J. Am. Chem. Soc.*, 2004, **126**, 12714–12715.
70 X. Ru, W. Shi, X. Huang, X. Cui, B. Ren and D. Ge, *Electrochim. Acta*, 2011, **56**, 9887–9892.
71 A. Rahman and M. K. Sanyal, *Adv. Mater.*, 2007, **19**, 3956–3960.
72 J. M. Velazquez, A. V. Gaikwad, T. K. Rout, J. Rzayev and S. Banerjee, *ACS Appl. Mater. Interfaces*, 2011, **3**, 1238–1244.
73 A. Wu, H. Kolla and S. K. Manohar, *Macromolecules*, 2005, **38**, 7873–7875.
74 A. Morozan, P. Jégou, S. Campidelli, S. Palacina and B. Jousselme, *Chem. Commun.*, 2012, **48**, 4627–4629.
75 G. Zhang, W. Yang and F. Yang, *J. Electroanal. Chem.*, 2007, **602**, 163–171.
76 G. Zhang, F. Yang and W. Yang, *React. Funct. Polym.*, 2007, **67**, 1008–1017.
77 S. Zhao, G. Zhang, L. Fu, L. Liu, X. Fang and F. Yang, *Electroanalysis*, 2011, **23**, 355–363.
78 S. Valarselvan and P. Manisankar, *Electrochim. Acta*, 2011, **56**, 6945–6953.
79 F. T. A. Vork and E. Barendrecht, *Electrochim. Acta*, 1990, **35**, 135–139.
80 S. Holdcroft and B. L. Funt, *J. Electroanal. Chem.*, 1988, **240**, 89–103.
81 Z. G. Qi and P. G. Pickup, *Chem. Commun.*, 1998, 15–16.
82 S. Y. Huang, P. Ganesan and B. N. Popov, *Appl. Catal., B*, 2009, **93**, 75–81.
83 S. Mokran, L. Makhloufi and N. Alonso-Vante, *J. Solid State Electrochem.*, 2008, **12**, 569–574.
84 Y. S. Choi, S. H. Joo, S. Lee, D. J. You, H. Kim, C. Pak, H. Chang and D. Seung, *Macromolecules*, 2006, **39**, 3275–3282.
85 S. M. Unni, V. M. Dhavale, V. K. Pillai and S. Kurungot, *J. Phys. Chem. C*, 2010, **114**, 14654–14661.
86 F. B. Su, Z. Q. Tian, C. K. Poh, Z. Wang, S. H. Lim, Z. L. Liu and J. Y. Lin, *Chem. Mater.*, 2010, **22**, 832–839.
87 R. A. Bull, F. R. Fan and A. J. Bard, *J. Electrochem. Soc.*, 1983, **130**, 1636–1638.
88 S. L. Gupta, D. Tryk, M. Daroux, W. Aldred and E. Yeager, *J. Electrochem. Soc.*, 1986, **133**, 120C.
89 C. Fabja, G. Frithum and H. Hartl, *Bunsen-Ges. Phys. Chem., Ber.*, 1990, **94**, 937–941.
90 W. Seeliger and A. Hamnett, *Electrochim. Acta*, 1992, **37**, 763–765.
91 M. Yuasa, A. Yamaguchi, H. Itsuki, K. Tanaka and M. Yamamoto, *Chem. Mater.*, 2005, **17**, 4278–4281.
92 R. Bashyam and P. Zelenay, *Nature*, 2006, **443**, 63–66.
93 A. L. M. Reddy, N. Rajalakshmi and S. Ramaprabhua, *Carbon*, 2008, **46**, 2–11.
94 K. Lee, L. Zhang, H. Lui, R. Hui, Z. Shi and J. J. Zhang, *Electrochim. Acta*, 2009, **54**, 4704–4711.
95 D. Nguyen-Thanh, A. I. Frenkel, J. Q. Wang, S. O'Brien and D. L. Akins, *Appl. Catal., B*, 2011, **105**, 50–60.
96 X. Yuan, X. Zeng, H. J. Zhang, Z. F. Ma and C. Y. Wang, *J. Am. Chem. Soc.*, 2010, **132**, 1754–1755.
97 W. Feng, H. Li, X. Cheng, T.-C. Jao, F.-B. Weng, A. Su and Y.-C. Chiang, *Appl. Surf. Sci.*, 2012, **258**, 4048–4053.
98 H. S. Oh, J. G. Oh, B. Roh, I. Hwang and H. Kim, *Electrochem. Commun.*, 2011, **13**, 879–881.
99 W. M. Millán, T. T. Thompson, L. G. Arriaga and M. A. Smit, *Int. J. Hydrogen Energy*, 2009, **34**, 694–702.
100 M. Yuasa, K. Oyaizu, H. Murata, K. Tanaka, M. Yamamoto and K. Ronbunshu, *Jpn. J. Polym. Sci. Technol.*, 2006, **63**, 601–606.
101 J. Chen, W. M. Zhang, D. Officer, G. F. Swiegers and G. G. Wallace, *Chem. Commun.*, 2007, 3353–3355.
102 W. M. Zhang, J. Chen, P. Wagner, G. F. Swiegers and G. G. Wallace, *Electrochem. Commun.*, 2008, **10**, 519–522.
103 H. S. Liu, Z. Shi, J. L. Zhang, L. Zhang and J. J. Zhang, *J. Mater. Chem.*, 2009, **19**, 468–470.
104 G. Wu, K. Artyushkova, M. Ferrandon, J. Kropf, D. Myers and P. Zelenay, *ECS Trans.*, 2009, **25**, 1299–1311.
105 E. Claude, T. Addou, J. M. Latour and P. Aldebert, *J. Appl. Electrochem.*, 1998, **28**, 57–64.
106 M. Yuasa, K. Oyaizu, H. Murata, K. Tanaka, M. Yamamoto and S. Sasaki, *Electrochemistry*, 2007, **75**, 800–806.
107 H. N. Cong, K. E. Abbassi and P. Chartier, *Electrochem. Solid-State Lett.*, 2000, **3**, 192–195.
108 H. N. Cong, K. E. Abbassi and P. Chartier, *J. Electrochem. Soc.*, 2002, **149**, 525–530.
109 H. N. Cong, K. E. Abbassia, J. L. Gautier and P. Chartier, *Electrochim. Acta*, 2005, **50**, 1369–1376.
110 R. M. G. Rajapakse, K. Murakami, H. M. N. Bandara, R. M. M. Y. Rajapakse, K. Velauthamurti and S. Wijeratne, *Electrochim. Acta*, 2010, **55**, 2490–2497.
111 A. U. Ranaweera, H. M. N. Bandara and R. M. G. Rajapakse, *Electrochim. Acta*, 2007, **52**, 7203–7209.
112 W. M. A. T. Bandara, D. M. M. Krishantha, J. S. H. Q. Perera, R. M. G. Rajapakse and D. T. B. Tennakoon, *J. Compos. Mater.*, 2005, **39**, 759–775.
113 R. M. G. Rajapakse, R. M. M. Y. Rajapakse, H. M. N. Bandara and B. S. B. Karunarathne, *Electrochim. Acta*, 2008, **53**, 2946–2952.
114 W. Bandara, D. M. M. Krishantha, J. Perera, R. M. G. Rajapakse and D. T. B. Tennakoon, *J. Compos. Mater.*, 2005, **39**, 759–775.
115 S. J. Higgins, H. L. Jones, M. K. McCart and T. J. Pounds, *Chem. Commun.*, 1997, 1907–1908.
116 K. Asazawa, K. Yamada, H. Tanaka, A. Oka, M. Taniguchi and T. Kobayashi, *Angew. Chem., Int. Ed.*, 2007, **46**, 8024–8027.
117 H. Y. Qin, Z. X. Liu, W. X. Yin, J. K. Zhu and Z. P. Li, *J. Power Sources*, 2008, **185**, 909–912.

118 T. S. Olson, S. Pylypenko, P. Atanassov, K. Asazawa, K. Yamada and H. Tanaka, *J. Phys. Chem. C*, 2010, **114**, 5049–5059.

119 Z. P. Li, Z. X. Liu, K. N. Zhu, Z. Li and B. H. Liu, *J. Power Sources*, 2012, **219**, 163–171.

120 H. Y. Qin, Z. X. Liu, L. Q. Ye, J. K. Zhu and Z. P. Li, *J. Power Sources*, 2009, **192**, 385–390.

121 H. Y. Qin, S. J. Lao, Z. X. Liu, J. K. Zhu and Z. P. Li, *Int. J. Hydrogen Energy*, 2010, **35**, 1872–1878.

122 H. Y. Qin, Z. X. Liu, S. J. Lao, J. K. Zhu and Z. P. Li, *J. Power Sources*, 2010, **195**, 3124–3129.

123 M. V. Anantha, V. V. Giridhar and K. Renuga, *Int. J. Hydrogen Energy*, 2009, **34**, 658–664.

124 H. Nguyen-Cong, V. de la Garza Guadarrama, J. L. Gautier and P. Chartier, *Electrochim. Acta*, 2003, **48**, 2389–2395.

125 H. Nguyen-Cong, V. de la Garza Guadarrama, J. L. Gautier and P. Chartier, *J. New Mater. Electrochem. Syst.*, 2002, **5**, 35–40.

126 J. L. Gautier, J. F. Marco, M. Gracia, J. R. Gancedo, V. de la Garza Guadarrama, H. Nguyen-Cong and P. Chartier, *Electrochim. Acta*, 2002, **48**, 119–125.

127 M. Malviya, J. P. Singh, B. Lal and R. N. Singh, *J. New Mater. Electrochem. Syst.*, 2005, **8**, 223–228.

128 R. N. Singh, B. Lal and M. Malviya, *Electrochim. Acta*, 2004, **49**, 4605–4612.

129 R. N. Singh, M. Malviya and P. Chartier, *J. New Mater. Electrochem. Syst.*, 2007, **10**, 181–186.

130 R. N. Singh, M. Malviya, M. M. Anindita, A. S. K. Sinha and P. Chartier, *Electrochim. Acta*, 2007, **52**, 4264–4271.

131 F. Y. Xie, Z. Q. Tian, H. Meng and P. K. Shen, *J. Power Sources*, 2005, **141**, 211–215.

132 İ. Becrik and F. Kadirgan, *Turk. J. Chem.*, 2001, **25**, 373–380.

133 Z. Y. Bai, L. Yang, L. Li, J. Lv, K. Wang and J. Zhang, *J. Phys. Chem. C*, 2009, **113**, 10568–10573.

134 F. T. A. Vork, L. J. J. Janssen and E. Barendrecht, *Electrochim. Acta*, 1986, **31**, 1569–1575.

135 K. Bouzek, K.-M. Mangold and K. Jüttner, *Electrochim. Acta*, 2000, **46**, 661–670.

136 K. Bouzek, P. Holzhauser, R. Kodym, S. Moravcova and M. Paidar, *J. Appl. Electrochem.*, 2007, **37**, 137–145.

137 M. H. Seo, E. J. Lim, S. M. Choi, H. J. Kim and W. B. Kim, *Top. Catal.*, 2010, **53**, 678–685.

138 D. J. Strike, N. F. De Rooij and M. Koudelkahep, *J. Appl. Electrochem.*, 1992, **22**, 922–926.

139 M. Ulmann, R. Kostecki, J. Augustynski, D. J. Strike and M. Koudelkahep, *Chimia*, 1992, **46**, 138–140.

140 S. Radhakrishnan and A. Adhikari, *J. Power Sources*, 2006, **155**, 157–160.

141 Y. W. Ma, S. J. Jiang, G. Q. Jian, H. S. Tao, L. S. Yu, X. B. Wang, X. Z. Wang, J. M. Zhu, Z. Hu and Y. Chen, *Energy Environ. Sci.*, 2009, **2**, 224–229.

142 J. C. Park and J. S. Kim, *Macromol. Res.*, 2002, **10**, 181–186.

143 H. B. Zhao, L. Li, J. Yang and Y. M. Zhang, *J. Power Sources*, 2008, **184**, 375–380.

144 S. Zhang, H. Wang, N. Zhang, F. D. Kong, H. Liu and G. P. Yin, *J. Power Sources*, 2012, **197**, 44–49.

145 V. Selvaraj and M. Alagar, *Electrochem. Commun.*, 2007, **9**, 1145–1153.

146 B. Qu, Y. T. Xu, S. J. Lin, Y. F. Zheng and L. Z. Dai, *Synth. Met.*, 2010, **160**, 732–742.

147 V. Selvaraj and M. Alagar, *Electrochem. Commun.*, 2007, **9**, 1145–1153.

148 Y. C. Zhao, X. L. Yang, J. N. Tian, F. Y. Wang and L. Zhan, *J. Power Sources*, 2010, **195**, 4634–4640.

149 H. B. Zhao, L. Li, J. Yang, Y. M. Zhang and H. Li, *Electrochem. Commun.*, 2008, **10**, 876–879.

150 H. B. Zhao, J. Yang, L. Li, H. Li, J. L. Wang and Y. M. Zhang, *Int. J. Hydrogen Energy*, 2009, **34**, 3908–3914.